PHR1 and PHL1 mediate rapid high-light responses and acclimation to triose phosphate oversupply

Lukas Ackermann[1], Monika Müller[1], Alina Johanna Hieber[1], Maria Klecker[1*]

[1] Plant Physiology, University of Bayreuth, 95440 Bayreuth, Germany

[*]Address correspondence to: Maria Klecker, Department of Plant Physiology, University of Bayreuth, Universitätsstrasse 30, D-95447 Bayreuth, Germany. e-mail: maria.klecker@uni-bayreuth.de

Short title: PHR1 and PHL1 signal photosynthetic stress

ORCID IDs

Maria Klecker 0000-0001-5508-2363

Lukas Ackermann 0009-0009-8604-6029

ABSTRACT

Fluctuations in light intensity require immediate metabolic adjustment which includes reprogramming of both plastidial and nuclear gene expression, but the signaling pathways behind such responses are not fully understood. Here we report the identification of an early high-light responsive pathway in *Arabidopsis thaliana* that depends on PHOSPHATE STARVATION RESPONSE 1 (PHR1) and PHR1-LIKE 1 (PHL1) transcription factors involved in low phosphate (P_i) signaling. High-light treatment rapidly induced the accumulation of PHR1-responsive transcripts in wildtype plants grown under nutrient-sufficient conditions, but not in *phr1 phl1* double knockout plants. Differences in starch accumulation and ATP levels were detected between wildtype and *phr1 phl1* mutants subjected to high light, suggesting a link between P_i signaling, carbohydrate partitioning, and energy status during stress. In line with a function of PHR1/PHL1 upon triose phosphate accumulation, we observed that blocking starch biosynthesis in the *phr1 phl1* double mutant, by introducing the *agd1-1* allele, causes a severe growth defect. Phenotypes of the *adg1 phr1 phl1* triple mutant such as high-light sensitivity and growth restriction in the absence of exogenously supplied sucrose resemble the previously described double mutant *adg1 tpt-2*, lacking a functional copy of the TRIOSE PHOSPHATE/PHOSPHATE TRANSLOCATOR (TPT), and we show that P_i responses are disturbed in *adg1 tpt-2*. We propose that P_i sequestration by photosynthesis and import of P_i into the chloroplast transiently depletes cytosolic P_i reserves upon sudden increases in light intensity. The low-P_i sensing machinery in the nucleus consequently implements early high-light transcriptional responses, qualifying P_i as a new operational retrograde signal.

Introduction

Light as a source of energy with highly fluctuating availability needs to be efficiently captured by the photoautotrophic metabolism. This necessitates an enzymatic machinery capable of coping with rapid changes in metabolic flux, as well as the containment of overexcitation-induced hazards. Both challenges are met not only by post-transcriptional regulation of enzyme activity (reviewed in König et al. (2012), Matiolli et al. (2022)), but also by pronounced changes in mRNA abundance that occur within 30 minutes upon an increase in irradiance (Vogel et al., 2014; Suzuki et al., 2015; Huang et al., 2019). The latter mechanism depends on fast signal transmission between the chloroplast and the nuclear transcription machinery. Such communication is mediated by ‘primary’ retrograde signals (Dietz, 2015),

48 including redox cues and reactive oxygen species like H_2O_2 and singlet oxygen which are
49 produced during photosynthetic reactions (Bechtold et al., 2008; Dietz et al., 2016).
50 Additionally, increased electron transport activity and light-induced Calvin cycle activation
51 promote the accumulation of primary products of carbon fixation (Dietz and Heber, 1984; Dietz
52 and Heber, 1986) which may themselves act as signaling molecules (Häusler et al., 2014; Moore
53 et al., 2014). Hence, induction of high-light specific gene expression partially depends on the
54 triose phosphate/phosphate translocator (TPT) that mediates the exchange of triose phosphates
55 or 3-phosphoglycerate (3-PGA) with inorganic phosphate (P_i) at the chloroplast envelope
56 (Schneider et al., 2002; Vogel et al., 2014; Weise et al., 2019). A central function of the TPT in
57 light acclimation and retrograde signaling was corroborated by the severe high-light dependent
58 phenotypes of double mutants defective in the *TPT* and *ADG1* (for *ADP GLUCOSE*
59 *PYROPHOSPHORYLASE 1*), encoding a small subunit of the ADP-glucose pyrophosphorylase
60 complex (AGPase) which is required for the biosynthesis of transitory starch (Schmitz et al.,
61 2012). Phenotypes of *adg1-1 tpt* double mutants include growth retardation, low diurnal
62 changes in carbohydrate levels, and high chlorophyll fluorescence. These observations point
63 towards an important role of photosynthate partitioning for retrograde signaling, however the
64 identity of the primary sensors as well as signal transduction mechanisms are still unclear.

65 Phosphorus makes up about 2-30 permille of the plant dry mass (Kumar et al., 2019), as it is
66 incorporated into a large subset of biomolecules. Systemic signaling of P_i availability and P_i
67 distribution within the plant body mainly depend on a conserved gene family encoding
68 PHOSPHATE STARVATION RESPONSE 1 (PHR1) and PHR1 LIKE (PHL) transcription
69 factors of the MYB coiled-coiled type (Rubio et al., 2001; Zhou et al., 2008; Bustos et al., 2010;
70 Thibaud et al., 2010; Sun et al., 2016). Simultaneous loss of *PHR1* and *PHL1* function affects
71 the expression of at least 68 percent of the P_i starvation responsive genes in the shoots of
72 Arabidopsis (*Arabidopsis thaliana)* (Bustos et al., 2010). A decrease in cellular P_i concentration
73 impairs production of the inositol pyrophosphate species InsP8, relieving PHR1/PHLs of
74 suppression by SPX (for SYG1/Pho81/XPR1) domain-containing proteins, thus linking
75 transcription factor activity to P_i availability (Puga et al., 2014; Dong et al., 2019; Zhu et al.,
76 2019; Ried et al., 2021). The transcriptional response to P_i scarcity leads to scavenging of
77 external and internal P_i sources through phosphatase induction (Morcuende et al., 2007) and
78 altered lipid metabolism (Misson et al., 2005; Pant et al., 2015b), anthocyanin biosynthesis
79 (Nilsson et al., 2012; Liu et al., 2022; Li et al., 2023), and protection from photodamage
80 (Nilsson et al., 2012), to name a selection. PHR1/PHLs are characterized as transcriptional
81 activators (Nilsson et al., 2007; Bustos et al., 2010). Accordingly, direct targets of PHR1

82 (Bustos et al., 2010; Castrillo et al., 2017) are strongly upregulated upon P_i starvation and
83 include genes such as *PHOSPHATE STARVATION-INDUCED GENE 2* (*PS2*; AT1G73010)
84 (Hanchi et al., 2018), *MONOGALACTOSYLDIACYLGLYCEROL SYNTHASE 3* (*MGD3*;
85 AT2G11810) (Kobayashi et al., 2004), and *GLYCEROPHOSPHODIESTER*
86 *PHOSPHODIESTERASE 1/SENESCENCE-RELATED GENE 3* (*SRG3*; AT3G02040) (Cheng
87 et al., 2011). Nevertheless, a subset of transcripts is specifically repressed under P_i-depleted
88 conditions which can be accounted for by the induction of microRNAs (reviewed in Paz-Ares
89 et al. (2022)), the induction of transcriptional repressors, as well as the modulation of genome
90 accessibility (Barragán-Rosillo et al., 2021) through PHR1/PHLs activity.

91 P_i is unique among the macronutrients in that it is the only root-supplied element which is
92 directly consumed by photosynthesis (Heldt and Rapley, 1970; Dietz and Heber, 1984). It has
93 been shown experimentally that under high-CO_2 and high-light conditions, photosynthesis can
94 indeed become limited by P_i supply to the chloroplast, both under P_i depleted and nutrient-rich
95 conditions (Dietz and Foyer, 1986; Sivak and Walker, 1986). However, whether rapid increase
96 in photosynthetic activity affects P_i homeostasis of the cell, is still unclear. In this study, we
97 show that increments in light intensity trigger an early nuclear transcriptional response
98 characteristic of P_i depletion which depends on *PHR1* and *PHL1*. Processes regulated by
99 PHR1/PHL1 upon increased illumination contribute to photosynthetic acclimation since
100 *phr1 phl1* mutants showed metabolic alterations compared to the wildtype when subjected to
101 high-light stress. Moreover, analysis of the starch biosynthesis-deficient *adg1 phr1 phl1* triple
102 mutant revealed an important function of P_i signaling when triose phosphate utilization is
103 impaired. Aspects of the growth defects observed for *adg1 phr1 phl1* phenocopy the *adg1 tpt-2*
104 mutant, suggesting that triose phosphate partitioning strongly affects P_i homeostasis. Together,
105 we propose that PHR1/PHL1 mediate rapid photosynthetic acclimation upon sudden increases
106 in light intensity by using P_i as a previously unknown operational retrograde signal.

107 # Results

108 **Acclimation to P_i starvation is disturbed in *adg1 tpt-2***

109 Photoassimilate allocation and utilization in the chloroplast and cytosol mainly
110 determine the rate of P_i recycling from photosynthetic products. To address how the partitioning
111 of phosphorylated assimilates affects P_i homeostasis, we examined the phenotypes of mutants
112 defective in starch biosynthesis (*adg1-1*) and chloroplastic triose phosphate export (*tpt-2*)
113 during P_i starvation in the presence of 14.61 mM (0.5 %) sucrose, and used anthocyanin
114 production as a read-out for the induction of the P_i starvation response. In accordance with
115 previous reports (Nilsson et al., 2007), wildtype seedlings accumulated anthocyanins when
116 transferred to P_i-deficient conditions (Figure 1A, B). This was not observed for the *phr1-3 phl1*
117 mutant. While *tpt-2* mutant seedlings were indistinguishable from the wildtype in terms of
118 anthocyanin content, pigmentation was significantly enhanced upon P_i starvation in *adg1-1*.
119 Surprisingly, this effect was fully reversed in the double mutant *adg1 tpt-2* which even
120 accumulated much lower amounts of anthocyanins than the wildtype (Figure 1B). Nevertheless,
121 root responses to P_i depletion such as root hair production were normal in *adg1 tpt-2* (Figure
122 1A). Hence, increased anthocyanin production of *adg1-1* upon P_i starvation almost fully relied
123 on photoassimilate transport over the chloroplast envelope. To test whether increased
124 anthocyanin accumulation in *adg1-1* also depends on the signaling pathway executed by
125 PHR1/PHLs, we created a triple mutant by crossing *adg1-1* and *phr1-3 phl1*. The anthocyanin
126 content did not increase in the *adg1 phr1 phl1* triple mutant in response to P_i starvation (Figure
127 1B), confirming a crucial function of PHR1/PHL1 signaling in this process even in the absence
128 of ADG1 activity.

129 P_i deprivation is also known to induce starch accumulation in a *PHR1*-dependent
130 manner (Figure 1C and Supplemental Figure 1), which likely involves AGPase activity (Nilsson
131 et al., 2007). Furthermore, also soluble sugar contents rise in wildtype plants upon P_i limitation
132 (Pant et al., 2015a). We reasoned that contrasting pigmentation behavior of the *adg1-1* and *adg1*
133 *tpt-2* seedlings under P_i-depleted conditions might be caused by differential sugar accumulation
134 (Zirngibl et al., 2023). First, we analyzed starch contents of seedling shoots under P_i-sufficient
135 and -deficient conditions. While shoots of *tpt-2* showed slightly higher levels of starch than
136 wildtype, P_i depletion did not result in considerable starch production in *adg1-1* or any of the
137 derived mutant lines (Figure 1C), confirming that the small AGPase subunit ADG1 is required
138 for increased starch accumulation under P_i starvation. In agreement with impaired starch
139 biosynthesis, hexose levels were increased in *adg1-1* shoots under P_i depletion compared to the

140 wildtype, and we observed a tendency towards higher sucrose levels in *adg1-1* (Figure 1C).
141 None of these effects were seen in the *adg1 phr1 phl1* triple mutant, suggesting that sugar
142 metabolism in *adg1-1* was under control of PHR1/PHL1 during P_i depletion (Figure 1C).
143 Surprisingly, sugar levels were not correlated to anthocyanin production in either *tpt-2* or *adg1*
144 *tpt-2*: While P_i-depleted shoots of *tpt-2* contained higher glucose levels than wildtype, the
145 contents of all three soluble sugar species analyzed were similar between shoots of *adg1 tpt-2*
146 and the wildtype when grown on sucrose-supplemented media (Fig. 1C). Thus, anthocyanin
147 production in response to P_i starvation was partially uncoupled from cellular sugar contents.
148 Taken together, PHR1/PHL1 activity is required, but not sufficient for anthocyanin production
149 under P_i starvation, which furthermore depends on adequate metabolite partitioning between
150 chloroplasts and the cytosol. Furthermore, the phenotypes of the *adg1 tpt-2* double mutant
151 indicate that P_i starvation responses are disturbed in this mutant.

152

153 **P_i starvation gene expression is triggered by high light**

154 The low-P_i phenotypes of *adg1-1* and *adg1 tpt-2* mutant lines indicated that P_i starvation
155 responses are affected by photoassimilate distribution and utilization. This raised the question
156 whether photoassimilate turnover also impacts on P_i homeostasis under non-starved conditions.
157 More specifically, P_i signaling might be modulated by naturally occurring changes in triose
158 phosphate metabolism, for example upon an increase in light intensity. To address this, we
159 tested low-P_i marker gene expression upon sudden increments in photon flux density. Using
160 quantitative RT-PCR (qRT-PCR), we first confirmed that in our experimental setup transcript
161 levels of *SRG3*, *PS2*, *SPX1*, and *MGD3* were all strongly induced by P_i starvation, which mainly
162 depended on *PHR1/PHL1* (Supplemental Figure 2A). Additionally, we analyzed transcript
163 levels of a putative vacuolar P_i efflux transporter, *VPE1* (AT3G47420) (Ramaiah et al., 2011;
164 Xu et al., 2019), and confirmed upregulation of this gene in the wildtype subjected to P_i
165 starvation which was again strongly attenuated in *phr1-1 phl1* mutants (Supplemental Figure
166 2A). Furthermore, for the promoter sequences of *SPX1* (lacking the naturally occurring *Nco*I
167 restriction site, $proSPX1^{GC}$), *MGD3*, and *SRG3*, we observed that PHR1 was able to induce the
168 expression of *promoter::LUC* fusion constructs when transiently expressed in mesophyll
169 protoplasts (Supplemental Figure 2B), confirming that *SPX1*, *MGD3*, and *SRG3* are targets of
170 PHR1.

171 To examine responses to enhanced illumination, we grew wildtype and *phr1-1 phl1*
172 mutant plants under nutrient-rich conditions on soil in an 8/16 hours (light/dark) photoregime.

173 After 5 weeks, photon flux density was increased to 320±30 µmol m^{-2} s^{-1} (high light) while the
174 control group was kept under growth light conditions of 80±5 µmol m^{-2} s^{-1}. Using qRT-PCR,
175 we detected a pronounced upregulation of *SRG3*, *SPX1*, and *VPE1* transcripts in wildtype plants
176 already after 20 min of exposure to high light compared to control plants, as well as a slight
177 increase in *MGD3* and *PS2* transcript abundance (Figure 2). In all five cases, the upregulation
178 of gene expression was attenuated within 125 min in high light (Figure 2), indicating that
179 response to P_i shortage constitutes an early consequence of increased irradiance. Notably,
180 induction of P_i starvation marker transcripts was not observed in *phr1-1 phl1* mutant plants
181 (Figure 2). *PHR1* expression itself was reported to depend on light (Liu et al., 2017).
182 Importantly however, increasing the light intensity to 320±30 µmol m^{-2} s^{-1} did not affect *PHR1*
183 transcript levels under our experimental conditions (Supplemental Figure 3), consistent with
184 the accumulation of *PHR1* transcript being only responsive to changes in the very low fluence
185 range (Liu et al., 2017).

186 *GLUCOSE-6-PHOSPHATE/PHOSPHATE TRANSLOCATOR 2* (*GPT2*) is a light
187 responsive gene (Athanasiou et al., 2010) which was also described to be induced by P_i
188 starvation (Morcuende et al., 2007). Furthermore, high-light induced expression of *GPT2* was
189 previously described to depend on *TPT* function (Kunz et al., 2010; Weise et al., 2019), and we
190 noted that the promotor sequence of *GPT2* contains a PHR1 binding motif (GTATATTC) close
191 to the transcriptional start site. Therefore, we tested if the *GPT2* promotor could be activated
192 by PHR1 in a transient expression system using the *LUC* reporter gene. In fact, *PHR1*
193 expression induced LUC reporter activity when protoplasts were co-transfected with the
194 *proGPT2::LUC*$_{Firefly}$ construct (Supplemental Figure 2B). However, the responsiveness of
195 *proGPT2* to *PHR1* expression was considerably lower than observed with the constructs
196 harboring *proSPX1*^{GC}, *proSRG3* or *proMGD3* upstream of the reporter CDS. Consistent with
197 weak PHR1-mediated induction of *proGPT2* in protoplast assays, and in contrast to the other
198 tested P_i-starvation responsive genes, *GPT2* was upregulated by high light in both wildtype and
199 *phr1-1 phl1* after 45 minutes, and transcript levels continued to rise upon stress during the
200 course of the analysis (Figure 2). This indicated that PHR1/PHL1 are not involved in high-light
201 mediated induction of *GPT2* expression. Moreover, we were not able to detect an effect of the
202 *gpt2-1* allele (Niewiadomski et al., 2005) on carbohydrate accumulation under P_i depletion
203 (Supplemental Figure 1), arguing against a major role of this gene for sugar homeostasis under
204 P_i starvation. Thus, metabolite transport over the chloroplast membrane likely creates another
205 signal which is responsible for *GPT2* induction under high light. While this pathway is not

206 affected by *phr1-1 phl1* mutation, the double mutant fails to induce other P_i-depletion
207 responsive genes which are upregulated in the wildtype very early after a shift in light intensity.

208

209 **Metabolic responses to increased light are impaired in *phr1 phl1* mutants**

210 Given that transcription of P_i-starvation responsive genes was rapidly induced by high
211 light, we asked if this response was of physiological significance during acclimation to
212 increased radiation. To investigate this, we determined the changes in adenylates, sugar, and
213 starch contents that occurred within 90 min upon an increase in photon flux density from
214 80±5 µmol m^{-2} s^{-1} to 320±30 µmol m^{-2} s^{-1} in rosette leaves of 5-weeks-old wildtype and
215 *phr1-1 phl1* mutant plants. As shown in Figure 3A, increasing the light intensity caused a slight
216 drop in ATP levels in leaves of *phr1-1 phl1* mutants, while no significant changes were seen in
217 wildtype plants. Notably, the ratio of ATP/ADP was not affected by either the genotype or the
218 high-light treatment (Figure 3A). In contrast, fructose, glucose, and sucrose levels increased in
219 leaves of both wildtype and *phr1-1 phl1* mutants subjected to high light as compared to control
220 light conditions (Figure 3B). Interestingly, total levels of glucose and fructose were slightly
221 lower in *phr1-1 phl1* leaves subjected to high light compared to wildtype leaves (Figure 3B).
222 However, the relative increments in sugar levels upon stress did not differ significantly between
223 wildtype and *phr1-1 phl1* mutants (Figure 3C).

224 Unlike sugar levels, starch content under control conditions was higher in *phr1-1 phl1*
225 mutants than in wildtype plants (Figure 3D). This may be related to the fact that *phr1-1 phl1*
226 mutants manifest lower P_i levels in the shoots (Wang et al., 2018a) which allosterically activates
227 AGPase (Figueroa et al., 2022). Exposure to higher light intensities further increased starch
228 content in both wildtype and *phr1-1 phl1* (Figure 3D). However, while the starch content of
229 wildtype leaves increased by 1.98-fold relative to control conditions, *phr1-1 phl1* mutant plants
230 exhibited a significantly lower increase by only 1.62-fold (Figure 3D). Thus, sequestration of
231 photoassimilates in transitory starch under high light conditions was affected by loss of
232 *PHR1/PHL1* function.

233 Since both P_i starvation and high-light stress trigger anthocyanin production, we next
234 analyzed the ability of *phr1 phl1* mutants to accumulate anthocyanins during high-light
235 acclimation. As shown in Figure 3E, anthocyanin contents of *phr1 phl1* leaves after 3 days of
236 high-light exposure were significantly lower than in wildtype leaves or in the single mutants
237 *phr1-3* and *phl1*, while loss of *SPX1/2* function did not have any statistically significant effect.
238 To exclude that *phr1 phl1* mutant plants were generally impaired in anthocyanin biosynthesis,

239 we subjected seedlings to chemically induced oxidative stress. Here, anthocyanin contents were
240 not significantly different between wildtype, *phr1-3 phl1*, and *spx1 spx2* seedlings after 5 days
241 of growth on paraquat-containing media (Supplemental Figure 4), indicating that anthocyanin
242 biosynthesis was functional during reactive oxygen stress in *phr1-3 phl1* mutants.

243 Next, we asked whether metabolic abnormalities in the *phr1 phl1* mutants were related
244 to differences in photosynthetic performance at the level of the thylakoid reactions. Therefore,
245 we performed pulse-amplitude modulated (PAM) chlorophyll fluorometry on rosette leaves
246 subjected to increased light. The efficiency of photosystem II photochemistry (ΦPSII) dropped
247 to the same extent in both wildtype and *phr1-1 phl1* mutants upon exposure to increased
248 illumination for 125 min (Figure 4A). After 125 min of treatment, also the maximum efficiency
249 of PSII (F_v/F_m) had decreased significantly in the stressed plants of both genotypes (Figure 4B).
250 As for ΦPSII, no difference was observed for F_v/F_m between wildtype and *phr1-1 phl1*. Thus,
251 *PHR1/PHL1* function likely affected adenylate levels, starch metabolism and anthocyanin
252 pigmentation of leaves under high-light stress in a manner independent of the thylakoid
253 reactions.

254

255 ***PHR1/PHL1* function is important when triose phosphate utilization is limited**

256 Our observations indicated that P_i-starvation signaling might be important during a shift
257 to higher light intensities. We hypothesized that this might be related to transient imbalances of
258 triose phosphate production and P_i recycling that occur upon changes in photosynthetic activity.
259 In order to address this, we tried to genetically mimic the otherwise transient state of insufficient
260 P_i recycling from photosynthetic products. In the *adg1-1* mutant, disruption of starch
261 biosynthesis leads to continuous limitation in triose phosphate utilization. Hence, we examined
262 the phenotypes of the *adg1 phr1 phl1* triple mutant to assess the importance of PHR1/PHL1
263 signaling during triose phosphate overaccumulation.

264 Strikingly, when grown under conditions with a short photoperiod (8 hours),
265 *adg1 phr1 phl1* mutant plants exhibited a strong growth defect that was apparent in a reduction
266 in both leaf size and leaf number compared to *adg1-1* single and *phr1-3 phl1* double mutants
267 (Figure 5A, B). Under long-day conditions (16 hours photoperiod), the reduction in rosette size
268 was less pronounced, but *adg1 phr1 phl1* mutant plants exhibited premature leaf senescence
269 with symptoms already visible at the age of 25 days (Figure 5A, arrow). Accelerated leaf
270 senescence is also seen in *phr1 phl1* double mutants particularly under P_i deprived conditions
271 (Bustos et al., 2010) (Figure 1A), but initiates later at the age of approximately 35 days when

272 grown under standard conditions on soil (Figure 5B) (Wang et al., 2018a). Furthermore,
273 transition to flowering was much delayed in *adg1 phr1 phl1* compared to the parental lines
274 (Figure 5C). Notably, delayed onset of the regenerative phase is a phenotype already inherent
275 to both the *adg1-1* (Matsoukas et al., 2013) and *phr1 phl1* (Supplemental Figure 5) mutants.

276 We noted that the photoperiod-dependent reduction in rosette size seen for
277 *adg1 phr1 phl1* was reminiscent of the phenotype of the *adg1 tpt-2* mutant (Figure 5A). Thus,
278 we tested the ability of *adg1 phr1 phl1* to adapt to higher light intensities, since high-light
279 sensitivity was also reported for the *adg1 tpt-2* mutant (Schmitz et al., 2012). In fact, seedling
280 shoot growth of *adg1 phr1 phl1* and *adg1 tpt-2* was reduced to a similar extent when grown
281 under high-light conditions (Figure 5D and Supplemental Figure 6). Moreover, growth of
282 *adg1 phr1 phl1* mutants under high light was promoted by exogenously supplied sucrose
283 (Figure 5D), as it was described for *adg1 tpt-2* (Heinrichs et al., 2012; Schmitz et al., 2012).
284 When seedlings were grown on vertically positioned petri dishes, it became evident that sucrose
285 strongly stimulated root growth of both *adg1 phr1 phl1* and *adg1 tpt-2* particularly under high-
286 light conditions (Supplemental Figure 7). Interestingly, when analyzing vertically grown
287 seedlings, we observed a tendency for high-light sensitivity of shoot growth also for the *adg1-*
288 *1* single and *phr1-3 phl1* double mutant lines (Supplemental Figure 6A). Likewise, this effect
289 could be alleviated by exogenously supplied sucrose. Notably, high-light sensitivity of *phr1-3*
290 *phl1* was more pronounced under high-P_i (2.5 mM) than low-P_i (0.25 mM) growth conditions
291 (Supplemental Figure 6A), supporting the hypothesis that PHR1/PHL1 play a role for high-
292 light adaptation also under P_i sufficiency. It was concluded from these experiments that lack of
293 *PHR1/PHL1* compromises plant growth under conditions of high triose phosphate
294 accumulation such as high light or when starch biosynthesis is genetically blocked.

295

296 **Carbohydrate signaling is affected during P_i deprivation**

297 Seedling growth of *phr1-3 phl1* (Supplemental Figure 6A) and *adg1 phr1 phl1* (Figure
298 5D and Supplemental Figure 7) was supported by sucrose supplementation particularly under
299 high light, and high-light induced starch accumulation was reduced in *phr1-1 phl1* mutants
300 (Figure 3D). Both observations suggest that *phr1 phl1* mutation leads to alterations in
301 carbohydrate metabolism. To address the question of how carbohydrate signaling might be
302 modulated under conditions when PHR1 activity is high, we re-analyzed published
303 transcriptome data obtained from seedlings subjected to P_i depletion (Bustos et al., 2010), and
304 from rosette plants exposed to a low CO_2 environment (Bläsing et al., 2005). Among the

305 transcripts which were most strongly upregulated in shoots of *phr1-1 phl1* under P_i depletion
306 relative to the wildtype, the majority was repressed by P_i depletion in the wildtype
307 (Supplemental Figure 8). This supports a function of PHR1/PHL1 in the downregulation of
308 certain transcripts under P_i depletion, as previously suggested (Bustos et al., 2010).
309 Interestingly, we noted that many of these transcripts were also responsive to carbon starvation
310 (Bläsing et al., 2005) (Supplemental Figure 8).

311 We chose four of the transcripts which were upregulated in *phr1-1 phl1* compared to
312 the wildtype under P_i starvation for further analysis: The circadian regulators *BASIC LEUCINE*
313 *ZIPPER 63* (*bZIP63*) (Baena-González et al., 2007; Frank et al., 2018) and *REVEILLE 1*
314 (*RVE1*) (Rawat et al., 2009), as well as *BETA-XYLOSIDASE1* (*BXL1*), and
315 *SENESCENCE1/DARK INDUCIBLE1* (*SEN1/DIN1*), a putative target gene of bZIP63
316 (Matiolli et al., 2011). In qRT-PCR analysis of seedlings grown on sucrose-containing media
317 with or without P_i, both *bZIP63* and *BXL1* were down-regulated in shoots of wildtype seedlings
318 exposed to P_i depletion, whereas no significant changes were detected for *phr1-1 phl1* mutants
319 (Figure 5E), potentially reflecting sugar accumulation in the wildtype (Supplemental Figure 1).
320 In contrast, transcript levels of *SEN1* and *RVE1* were highly increased in *phr1-1 phl1* mutants
321 under P_i deprivation, but no significant changes were seen in the wildtype background (Figure
322 5F). Thus, expression of carbohydrate responsive genes, including circadian-clock associated
323 genes, differs between wildtype and *phr1-1 phl1* mutants under P_i depletion.

324

325 **Transcription in the *adg1 tpt-2* mutant exhibits a constitutive P_i-starvation signature**

326 The phenotypic similarities of the *adg1 phr1 phl1* and *adg1 tpt-2* mutants suggested that
327 triose phosphate partitioning and P_i signaling share some physiological consequences,
328 supporting that triose phosphate utilization affects cellular P_i homeostasis. To assess if
329 PHR1/PHLs activity was altered in *adg1 tpt-2*, we analyzed P_i-starvation marker gene
330 expression in rosette leaves of plants grown for 5 weeks under an 8-hours light regime and a
331 moderate light intensity of 90±10 $\mu mol\ m^{-2}\ s^{-1}$. Surprisingly, *SRG3*, *PS2*, *SPX1*, *VPE1* and
332 *MGD3* were all significantly upregulated in shoots of soil-grown *adg1 tpt-2* plants compared
333 to wildtype or the single *adg1-1* and *tpt-2* mutants (Figure 6A), indicating high activity of PHR1
334 in shoots of *adg1 tpt-2*. Moreover, *bZIP63* expression was significantly reduced in both *adg1-1*
335 and *adg1 tpt-2*, whereas we observed a slight increase in *bZIP63* transcript levels in rosette
336 leaves of *tpt-2* mutants (Figure 6A). To test if altered expression of P_i-starvation associated
337 genes in *adg1 tpt-2* was linked to reduced P_i levels in the shoots of the mutant, we next

338 determined P_i contents in 5-weeks-old rosette leaves grown on soil under moderate light.
339 Interestingly, the P_i content was not reduced in shoots of *adg1 tpt-2* compared to the wildtype,
340 but P_i levels were even found to be higher than in *adg1-1* single mutants (Figure 6B). Thus, P_i
341 loading of the shoots was not impaired in *adg1 tpt-2*, and P_i-starvation responsive genes were
342 instead constitutively upregulated in *adg1 tpt-2* rosette leaves, indicating high PHR1 activity
343 even under nutrient-sufficient physiological conditions in this mutant.

344

345 Discussion

346 The observations presented herein establish that the P_i response machinery involving
347 the transcription factors PHR1 and PHL1 is capable of sensing early high-light stress, and we
348 provide evidence that *PHR1/PHL1* contribute to the rapid adjustment of carbohydrate
349 metabolism during changes in light intensity. P_i consumption by photosynthesis is thus
350 hypothesized to generate a chloroplast-to-nucleus retrograde signal. In fact, P_i qualifies as a
351 subcellular signal by a number of criteria: 1) [P_i] changes immediately and gradually in response
352 to photoassimilation (Stitt et al., 1980; Dietz and Heber, 1984; Robinson and Giersch, 1987);
353 2) multiple transport proteins at the organellar membranes (Fabiańska et al., 2019) ensure rapid
354 transmission of the [P_i] signal; 3) signal propagation is based on diffusion and does not rely on
355 acceptor and donor molecules; 4) P_i exhibits low toxicity within a wide concentration range; 5)
356 a highly responsive signaling machinery is present in the cytosol and nucleus.

357

358 Increase in light intensity creates a transient low-P_i signal

359 Under conditions where carboxylation exceeds subsequent metabolic capacities of the
360 chloroplast, such as high light (Laisk et al., 1991), low temperature (Stitt and Grosse, 1988),
361 and low oxygen (Klecker et al., 2014), large pools of 3-phosphoglycerate may build up which
362 can enter the cytosol via the TPT (Schneider et al., 2002). By the nature of the transport
363 mechanism, this depletes the cytosol of P_i, and it is assumed that P_i import from the vacuole is
364 too slow to balance against very short-term changes in P_i demand (Woodrow et al., 1984). In
365 accordance with these considerations, we found that transcription exhibits a P_i-starvation
366 signature in Arabidopsis rosette leaves subjected to light increase already after 20 min of stress
367 (Figure 2). This response depended on *PHR1/PHL1* function, indicating that light stress
368 activated the cytosolic and nuclear P_i sensing machinery (Figure 7). PHR1 target genes which
369 showed enhanced expression in our experimental setup included *SRG3*, *SPX1*, and *VPE1*, and

370 all three transcripts also showed early enrichment upon high-light treatment within a time-
371 resolved transcriptome analysis previously described by Huang et al. (2019). Both *SRG3* and
372 *VPE1* expression might be suitable to rapidly increase P_i availability in the cytosol via
373 glycerophosphodiester turnover (Cheng et al., 2011) and vacuolar P_i efflux (Xu et al., 2019),
374 respectively. In contrast, *SPX1* upregulation potentially contributes to the rapid tempering of
375 the transcriptional response which was quenched already after 2 hours of treatment (Figure 2).
376 Next to negative feed-back by SPX1, adjustment of triose phosphate turnover by post-
377 translational activation of sucrose (Stitt et al., 1983; Preiss, 1984) and starch (Preiss, 1988;
378 Hendriks et al., 2003) biosynthesis would be expected to attenuate any condition of light-
379 induced P_i depletion within relatively short time. Therefore, long-term P_i-starvation responses
380 such as lipid remodeling are rather unlikely to occur upon light intensity increases as long as
381 higher P_i demand can be sufficiently covered by uptake via the roots or release of P_i storage
382 within the mesophyll cell. Consistent with this assumption, induction of *MGD3* transcript was
383 moderate in our experimental setup (Figure 2). Interestingly however, van Rooijen et al. (2018)
384 observed upregulation of PHR1 target genes with involvement in lipid remodeling after 1 hour
385 of irradiance increase. Thus, it will be exciting to learn from future experiments whether P_i
386 signaling also contributes to the changes that can be seen in the lipid composition of leaves
387 under different light conditions (Yu et al., 2021).

388

389 **P_i sensing impacts on carbohydrate and energy metabolism upon light increase**

390 The induction of genes related to P_i mobilization upon high light might be considered a
391 transcriptional feedback response initiated in order to sustain substrate supply for metabolic
392 reactions. Classification of P_i as a retrograde signal requires, beyond that, P_i signaling to affect
393 further physiological processes by calibrating nuclear gene expression according to the status
394 of the plastids. Crucially, this study shows that mutants defective in *PHR1* and *PHL1* which
395 fail to mount a transcriptional response related to P_i starvation, develop metabolic abnormalities
396 in the leaves within only 1.5 hours of high-light treatment (Figure 3A-D), and exhibit lower
397 levels of anthocyanin pigmentation after 3 days of treatment (Figure 3E). ATP levels measured
398 after 1.5 hours of high-light exposure were significantly lower in leaves of *phr1-1 phl1* mutant
399 plants compared to wildtype plants (Figure 3A), whereas ΦPSII values were indistinguishable
400 (Figure 4A). Given that ΦPSII can be interpreted as a measure of the linear electron transport
401 rate (Maxwell and Johnson, 2000), this indicates that ATP synthesis at the thylakoids was likely
402 not affected by loss of *PHR1/PHL1* function. This is consistent with the assumption that P_i

403 sequestration upon photosynthetic activity does not compromise stromal P_i levels and thus ATP
404 synthesis as long as phosphorylated metabolites are exchanged with the cytosol via P_i antiport
405 systems (Robinson and Giersch, 1987). In contrast, it would be conceivable that the P_i
406 concentration outside of the chloroplast might drop below levels required for efficient
407 mitochondrial ATP synthesis in the *phr1-1 phl1* mutant. In fact, a decline in ATP levels can
408 also be observed in plants under P_i-deficient growth conditions (Zhu et al., 2019; Riemer et al.,
409 2021), but the reason for this is currently unknown.

410 While starch levels under standard light conditions were slightly higher in *phr1-1 phl1*
411 rosettes compared to wildtype, the high-light induced relative increase in starch content was
412 considerably higher in wildtype leaves compared to the mutant (Figure 3D). This delay in the
413 activation of starch biosynthesis is remarkable, given that post-translational activation of
414 AGPase by the 3-PGA/P_i ratio is probably high in *phr1-1 phl1* leaves which manifest
415 chronically low P_i contents (Wang et al., 2018a). Similar to what can be seen under P_i
416 deprivation (Supplemental Figure 1) (Nilsson et al., 2007), the difference in starch
417 accumulation observed between wildtype and *phr1-1 phl1* mutants upon transfer to high light
418 was not reflected by changes in soluble sugar contents (Figure 3B, C). Together with our finding
419 that photosynthetic capacity is wildtype-like in *phr1-1 phl1* mutants subjected to high-light
420 stress (Figure 4), this suggests that starch production is rather not limited by photosynthetic
421 precursor production in *phr1-1 phl1*. Hence, it is likely that PHR1/PHL1 directly regulate
422 photoassimilate partitioning towards starch biosynthesis. Expression of *APL3* (AT4G39210)
423 encoding a large subunit of AGPase, or *GGBS1* (AT1G32900), coding for a granule-bound
424 starch synthase have been described to be induced by P_i starvation (Morcuende et al., 2007;
425 Bustos et al., 2010; Wang et al., 2018b), and might contribute to both P_i-starvation and high-
426 light induced starch accumulation.

427

428 **P_i signaling is crucial under conditions of triose-phosphate oversupply**

429 Prevention of starch production during P_i restriction leads to higher sugar and
430 anthocyanin levels in the shoots (Figure 1). The observation is consistent with sugars being
431 formed upon recycling of phosphorylated metabolites (Morcuende et al., 2007), and starch
432 serving as a carbon sink in P_i-deprived plants (Hammond and White, 2008; MacNeill et al.,
433 2017). Neither sugar accumulation, nor transitory starch or anthocyanin production take place
434 in *phr1 phl1* mutant seedlings subjected to P_i depletion (Figure 1 and Supplemental Figure 1).
435 Nevertheless, prohibition of starch biosynthesis by introduction of the *adg1-1* allele into this

436 mutant background produced a pronounced growth defect already visible at the seedling stage
437 (Figure 5A, B, D and Supplementary Figures 6, 7). Growth of the *adg1 phr1 phl1* triple mutant
438 was further impaired by higher light intensities (Figure 5D and Supplemental Figure 6), a
439 condition that reinforces triose phosphate generation. These observations lead to the conclusion
440 that *PHR1/PHL1* function is crucial in the *adg1-1* knockout situation, demonstrating the
441 necessity for low-P_i signaling when photoassimilate consumption is constrained. Next to
442 growth retardation, the *adg1 phr1 phl1* mutant showed a delay in the onset of flowering (Figure
443 5C), and benefited from exogenous sucrose supply in terms of both shoot and root growth
444 (Figure 5D and Supplemental Figures 6, 7). Both late flowering (Wahl et al., 2013) and
445 inhibition of primary root growth (Smith and Stitt, 2007) indicate that *adg1 phr1 phl1* plants
446 suffer from carbohydrate starvation in the absence of external sucrose supply.

447 Interestingly, transcriptional changes observed on wildtype and *phr1-1 phl1* mutant
448 plants under P_i deprivation also indicate that PHR1/PHL1 maintain sugar homeostasis when P_i
449 availability is low (Figure 5E, F and Supplemental Figure 8). In agreement, strong increments
450 in the levels of amino acids and oligosaccharides such as raffinose and kestose were reported
451 for wildtype but not *phr1* mutants under P_i depletion (Pant et al., 2015a). Notably,
452 oligosaccharide production facilitated by PHR1/PHL1 might serve as an alternative
453 carbohydrate sink in the *adg1-1* mutant, and could support carbon supply of the starchless
454 mutant during the night. This would be consistent with the observation that *adg1 phr1 phl1* was
455 more strongly constrained by diel cycles with short light phases (Figure 5A). Similarly,
456 oligosaccharide and amino acid accumulation triggered by the low-P_i signaling module could
457 support carbohydrate homeostasis during high-light stress by maintaining P_i/C(/N) balance, and
458 might even be suitable to prepare for potential osmotic stress as a likely consequence of high
459 light in a natural environment. In line with this, a function of PHR1/PHL1 in proline
460 accumulation and drought resistance has been reported (Aleksza et al., 2017; Scheible et al.,
461 2023). It is difficult to dissect direct effects of P_i signaling from secondary consequences of P_i-
462 deprived metabolism. Thus, metabolic differences of *adg1 phr1 phl1* mutants grown under
463 short and long photoperiods might reveal new insights into how carbon fluxes are modulated
464 by P_i signaling.

465

466 **P_i signaling is affected in *adg1 tpt-2***

467 Strikingly, growth defects and high-light sensitivity of *adg1 phr1 phl1* are paralleled by
468 the phenotypes of the *adg1 tpt-2* mutant (Figure 5A, D and Supplemental Figures 6, 7),

469 indicating that photoassimilate allocation and P_i signaling to some extent overlap in terms of
470 their physiological consequences. Even under P_i sufficient growth conditions, we found that
471 *adg1 tpt-2* exhibits a signature of P_i-starvation responsive gene expression (Figure 6), raising
472 the question how insufficient export of photosynthetic products could generate a situation of
473 high PHR1 activity. In the *adg1 tpt-2* mutant, a pronounced fraction of cytosolic/chloroplastic
474 P_i can be assumed as metabolically unavailable, given that starch biosynthesis is prevented by
475 *adg1-1* mutation, while sucrose production during the course of the day remains at much lower
476 levels compared to *adg1-1* (Schmitz et al., 2012) (Figure 7). Hence, bulk release of P_i in *adg1*
477 *tpt-2* might be restricted to glycolysis and vacuolar phosphatase activity acting on
478 phosphorylated intermediates such as phosphoenolpyruvate (Ohnishi et al., 2018). This would
479 cause unequal intracellular pool sizes of free P_i, facilitating PHR1 activity in the
480 cytosol/nucleus, while vacuolar P_i stores are high (Figure 6).

481 In fact, imbalances of intracellular P_i pools would affect both *PHR1*-dependent and
482 independent (Osorio et al., 2019; Nam et al., 2021) P_i-responsive pathways. Such inadequate
483 signaling could even contribute to the pleiotropic defects observed for *adg1 tpt-2* mutants
484 (Schmitz et al., 2012), for example by altering lipid composition, or by the regulation of
485 photosynthesis-associated genes (Morcuende et al., 2007; Bustos et al., 2010; Barragán-Rosillo
486 et al., 2021; Nam et al., 2021). Interestingly, we also found that transcript levels of the circadian
487 regulator bZIP63 were downregulated both by P_i depletion (Figure 5E), and in the *adg1 tpt-2*
488 mutant (Figure 6). Given that *adg1 tpt-2* is characterized by overall low carbohydrate levels
489 (Schmitz et al., 2012), *bZIP63* expression appears to be uncoupled from sugar levels in this
490 mutant situation. Our observations open up the possibility that P_i signaling could be involved
491 in this regulation which will be an exciting topic to address in the future.

492

493 **Conclusions**

494 High-light stress requires immediate responses to avert damage to cellular components.
495 As a potential mode of sensing excess photosynthetic activity, we describe a function of the P_i-
496 sensing machinery involving PHR1 and PHL1 transcription factors under nutrient replete
497 growth conditions. We propose that P_i sequestration into phosphorylated photoassimilates and
498 metabolite exchange across the chloroplast membrane causes transient P_i restriction in the
499 cytosol and nucleus. This activates PHR1/PHL1 proteins to mobilize cellular P_i and to support
500 acclimation responses such as starch biosynthesis. The finding that P_i signaling is disturbed in

501 the *adg1 tpt-2* mutant emphasizes that PHR1/PHL activity constitutes a so-far underestimated
502 contributor to retrograde signaling of photosynthetic status.

503

504 Materials and Methods

505 Plant material

506 All Arabidopsis plants used in this study are in the background of the Columbia-0
507 accession. The *phr1-3* (AT4G28610; SALK_067629C) (Nilsson et al., 2007) and *phl1*
508 (AT5G29000; SAIL_731_B09) (Klecker et al., 2014) lines were described previously and the
509 derived homozygous double mutant *phr1-3 phl1* was a kind gift of Angelika Mustroph
510 (University of Bayreuth). The double mutant *phr1-1 phl1* (Bustos et al., 2010) was backcrossed
511 to *phl1* in order to remove a transgene containing the *NPTII* cassette which was previously
512 introduced for isolation of the *phr1-1* allele (Rubio et al., 2001). All experiments were
513 performed with the homozygous double mutant *phr1-1 phl1* lacking the *NPTII* cassette. The
514 double mutant *spx1 spx2* was described earlier (Puga et al., 2014). Knockout lines *adg1-1*
515 (At5g48300) (Lin et al., 1988), *tpt-2* (At5g46110; SALK_073707.54.25.x) and *adg1 tpt-2*
516 (Schmitz et al., 2012) were kindly provided by Rainer E. Häusler (University of Cologne).
517 *gpt2-1* (AT1G61800; GK-454H06) was obtained from The Nottingham Arabidopsis Stock
518 Centre (NASC) and was described previously (Niewiadomski et al., 2005). Primer sequences
519 used for genotyping are listed in Table S1. Homozygous insertion mutants were verified using
520 the following primer combinations: *PHR1* WT: PHR1_F/PHR1_R; *phr1-3* T-DNA:
521 LBb1/PHR1_R; *PHL1* WT: PHL1_F/PHL1_R; *phl1* T-DNA: PHL1_F/LB3; *TPT* WT:
522 TPT_F/TPT_R; *tpt-2* T-DNA: *tpt-2*_F/LBb1; *GPT2* WT: GPT2_F/GPT2_R; *gpt2-1* T-DNA:
523 GK-LB/GPT2_R. To generate the *adg1 phr1 phl1* triple mutant, *adg1-1* was crossed to *phr1-3*
524 *phl1*. Homozygous *adg1-1* mutants were identified by screening for starch-free phenotypes by
525 iodine staining at the end of the photoperiod. Homozygosity of the *phr1-1* allele was verified
526 by Sanger sequencing (Macrogen Europe, Amsterdam) of the PCR product of
527 PHR1_F/PHR1_R using primer PHR1_R.

528

529 Cultivation conditions

530 Seeds were stratified for 64 hours at 4°C in the dark. For vegetative growth, plants were
531 germinated and grown in an 8 h/16 h (light/dark) cycle on soil consisting of seeding compost,
532 universal soil, and vermiculite mixed in a 3:3:1 ratio. For high-light experiments, the plants

533 were additionally fertilized once directly after pricking at the age of 10 days using a complete
534 mineral mixture (Wuxal Super, Aglukon Spezialduenger, Duesseldorf, Germany) according to
535 the manufacturer's instructions. For seedling experiments, seeds were surface sterilized by
536 chlorine gas exposure and transferred to solidified Arabidopsis growth media as described in
537 the figure legends. Seedlings were grown under 16 h/8 h light/dark cycles. For paraquat
538 treatments, seedlings were germinated on agar-solidified media containing full-strength
539 Murashige and Skoog (MS) salts and grown for 10 days before transfer to MS media with or
540 without 1 µM paraquat dichloride hydrate (#36541, Riedel-de Haën, Hannover, Germany). If
541 not indicated otherwise, growth light was set to 90±10 µmol m^{-2} sec^{-1} and monitored using an
542 illuminance meter.

543

544 **P_i-starvation experiments**

545 For P_i-starvation experiments, seeds were germinated on medium containing MS salts
546 at full strength together with 0.8 % (w/v) phytoagar (Duchefa Biochemie, Haarlem, The
547 Netherlands) and 0.5 % (w/v) sucrose. After 5-10 days of growth (see figure legends), seedlings
548 were transferred to P_i media (0.5 % (w/v) sucrose; 20 mM 2-(N-Morpholino)-ethane sulphonic
549 acid; 2.5 mM KNO_3; 1 mM $MgSO_4$; 1 mM $Ca(NO_3)_2$; 2.5 mM KH_2PO_4; 25 µM Fe-EDTA;
550 35 µM H_3BO_3; 7 µM $MnCl_2$; 0.25 µM $CuSO_4$; 0.5 µM $ZNSO_4$; 0.1 µM $NaMoO_4$; 5 µM NaCl;
551 0.005 µM $CoCl_2$; pH 6) solidified by 0.8 % (w/v) agar (adopted from Härtel et al. (2000)). For
552 P_i depleting conditions, KH_2PO_4 was omitted, and Fe-EDTA was reduced to 10 µM in order to
553 minimize low-P_i induced iron toxicity (Ward et al., 2008). Seedling shoots were harvested after
554 7-8 days of growth on P_i differing media (see figure legends). For horizontally grown seedlings,
555 MS salts were used at ½ concentrations and 0.6 % (w/v) agar were applied. For the experiment
556 shown in Figures S6 and S7, P_i medium was used containing either 0.25 mM KH_2PO_4/10 µM
557 Fe-EDTA, 2.5 mM KH_2PO_4/25 µM Fe-EDTA, or 2.5 mM KH_2PO_4/25 µM Fe-EDTA +50 mM
558 sucrose.

559

560 **Vector construction**

561 Standard molecular cloning procedures were applied. Primer sequences used for cloning
562 are listed in table S1. The firefly *LUCIFERASE* reporter plasmid *pBT10-proMGD3::LUC*$_{Firefly}$
563 and the *pHBTL-p35S::3HA-GFP* effector plasmid (Klecker et al., 2014), as well as the *pBT10-*
564 *p35S::LUC*$_{Renilla}$ normalization plasmid (Bäumler et al., 2019) have been described elsewhere.

565 For details on cloning *proSPX1*^{GC}, *proSRG3*, *proMGD3*, *proGPT2,* and the *PHR1* effector
566 construct, refer to the supplemental methods.

567

568 **Anthocyanin determination**

569 Anthocyanin contents were determined with few changes as described in
570 (Vandenbussche et al., 2007). In brief, 40-70 mg of seedling shoots or rosette leaf material were
571 frozen in liquid nitrogen and ground in a bead mill (MM400, Retsch, Haan, Germany). The
572 frozen powder was resuspended in 300 µl of methanol containing 1 % HCl. After vortex-mixing
573 for 15 sec, cell debris was pelleted by centrifugation for 15 min at >14,000 g, 4°C. The
574 supernatant was mixed with 200 µl water and 500 µl chloroform by vortexing for 15 sec. After
575 15 min centrifugation at 17,900 g, 4°C, the upper phase was diluted in methanol to measure the
576 absorbance at 535 nm and 630 nm using a spectrophotometer (Specord 200 Plus, Analytik Jena,
577 Jena, Germany).

578

579 **Measurements of starch, soluble sugars, and adenylates**

580 Carbohydrates were determined by the Warburg optical test and adenylates were
581 assessed based on luciferase activity. Both procedures were described previously (Mustroph et
582 al., 2006), for details see supplemental methods.

583

584 **Determination of P_i contents**

585 Free P_i was determined in leaf tissue based on the method described by (Ames, 1966)
586 with some modifications partially based on (Sakuraba et al., 2018). For detail see supplemental
587 methods.

588

589 **RNA extraction and cDNA synthesis**

590 Plant material was harvested under the respective experimental conditions and instantly
591 frozen in liquid nitrogen. The tissue was ground in a bead mill, and RNA was extracted using
592 Bioline TRIsure (Meridian Bioscience, Cincinnati, United States) according to the
593 manufacturer's instructions. The quality of the RNA was assessed by screening A_{260} and A_{280}.
594 For qRT-PCR analysis, 1 µg of RNA was treated with DNAse I (Thermo Fisher Scientific,
595 Waltham, United States) according to product instructions before application in reverse

596 transcription using oligo(dT)$_{15}$ and RevertAid Reverse Transcriptase (Thermo Fisher
597 Scientific). Complementary DNA was diluted by a factor of 50 for use as template in qPCR
598 analysis. qPCR was performed in technical triplicates using SsoAdvanced Universal SYBR
599 Green Supermix (Bio-Rad, Hercules, United States) on a CFX Connect Real-time System (Bio-
600 Rad). Transcript levels were normalized to the levels of *PP2A* transcript and calculated as
601 $1000 \cdot 2^{-\Delta CT}$. Primer sequences are listed in table S1.

602

603 **Protoplast isolation, transfection and transactivation assay**

604 Leaf mesophyll protoplasts were isolated using the "Tape-Arabidopsis Sandwich"
605 method (Wu et al., 2009) with minor modifications. For details, see supplemental methods.

606

607 **Chlorophyll fluorescence measurements**

608 For the determination of the quantum yield of photosystem II photochemistry
609 $(F_m'-F')/F_m'$ (ΦPSII), as well as the maximum efficiency of photosystem II (F_v'/F_m'), pulse-
610 amplitude-modulated fluorescence measurements (PAM) of chlorophyll fluorescence were
611 conducted using a Junior-PAM (Walz, Effeltrich, Germany). Here, to calculate chlorophyll
612 fluorescence parameters using the saturating pulse method (Schreiber et al., 1986), one large
613 rosette leaf was held between two magnets and subjected to 10 seconds of actinic light
614 irradiance set to control light intensity (80±5 µmol m^{-2} sec^{-1}), followed by a saturation light
615 pulse.

616

617 **Statistical analysis**

618 Statistical analyses were performed with Microsoft Office Excel using the Real
619 Statistics Resource Pack software (www.real-statistics.com).

620

621 Funding information

622 This research was funded by the University of Bayreuth.

623 # Acknowledgements

624 We thank Stephan Clemens and Angelika Mustroph for helpful discussions and
625 comments on the manuscript, as well as for providing infrastructure and equipment. We thank
626 Kristina Munzert for help with experiments.

627

628 # Author contributions

629 M. K. designed the research, analyzed data, and wrote the paper; L. A., M. M., A. H.,
630 and M. K. performed research.

631

632 # Supplemental Data

633 **Supplemental Figure 1** Changes in sugar and starch contents under P_i depletion.

634 **Supplemental Figure 2** Expression of selected P_i-starvation responsive genes is activated by
635 PHR1/PHL1.

636 **Supplemental Figure 3** *PHR1* transcript levels are not affected by short-time high-light
637 exposure.

638 **Supplemental Figure 4** Anthocyanin production of P_i signaling mutants under ROS stress.

639 **Supplemental Figure 5** Delayed onset of flowering in *phr1-1 phl1* mutants.

640 **Supplemental Figure 6** Quantification of shoot fresh weights of seedlings grown under low
641 and high light.

642 **Supplemental Figure 7** Root growth of *adg1 phr1 phl1* and *adg1 tpt-2* responds to
643 exogenously supplied sucrose.

644 **Supplemental Figure 8** Carbohydrate responsive gene expression is affected under P_i
645 starvation.

646 **Supplemental Table 1** List of primer sequences used in this study.

647 **Supplemental Methods**

648

649 # REFERENCES

650 **Aleksza D, Horváth G V., Sándor G, Szabados L** (2017) Proline accumulation is regulated
651 by transcription factors associated with phosphate starvation. Plant Physiol **175**: 555–567

652 **Ames BN** (1966) [10] Assay of inorganic phosphate, total phosphate and phosphatases.
653 Methods Enzymol. pp 115–118

654 **Athanasiou K, Dyson BC, Webster RE, Johnson GN** (2010) Dynamic acclimation of
655 photosynthesis increases plant fitness in changing environments. Plant Physiol **152**: 366–
656 73

657 **Baena-González E, Rolland F, Thevelein JM, Sheen J** (2007) A central integrator of
658 transcription networks in plant stress and energy signalling. Nature **448**: 938–42

659 **Barragán-Rosillo AC, Peralta-Alvarez CA, Ojeda-Rivera JO, Arzate-Mejía RG, Recillas-**
660 **Targa F, Herrera-Estrella L** (2021) Genome accessibility dynamics in response to
661 phosphate limitation is controlled by the PHR1 family of transcription factors in
662 Arabidopsis. Proc Natl Acad Sci U S A **118**: e2107558118

663 **Bäumler J, Riber W, Klecker M, Müller L, Dissmeyer N, Weig AR, Mustroph A** (2019)
664 AtERF#111/ABR1 is a transcriptional activator involved in the wounding response. Plant
665 J **100**: 969–990

666 **Bechtold U, Richard O, Zamboni A, Gapper C, Geisler M, Pogson B, Karpinski S,**
667 **Mullineaux PM** (2008) Impact of chloroplastic- and extracellular-sourced ROS on high
668 light-responsive gene expression in Arabidopsis. J Exp Bot **59**: 121–33

669 **Bläsing OE, Gibon Y, Günther M, Höhne M, Morcuende R, Osuna D, Thimm O, Usadel**
670 **B, Scheible W-R, Stitt M** (2005) Sugars and circadian regulation make major
671 contributions to the global regulation of diurnal gene expression in Arabidopsis. Plant Cell
672 **17**: 3257–81

673 **Bustos R, Castrillo G, Linhares F, Puga MI, Rubio V, Pérez-Pérez J, Solano R, Leyva A,**
674 **Paz-Ares J** (2010) A central regulatory system largely controls transcriptional activation
675 and repression responses to phosphate starvation in Arabidopsis. PLoS Genet **6**: e1001102

676 **Castrillo G, Teixeira PJPL, Paredes SH, Law TF, de Lorenzo L, Feltcher ME, Finkel OM,**
677 **Breakfield NW, Mieczkowski P, Jones CD, et al** (2017) Root microbiota drive direct
678 integration of phosphate stress and immunity. Nature **543**: 513–518

679 **Cheng Y, Zhou W, El Sheery NI, Peters C, Li M, Wang X, Huang J** (2011) Characterization

680 of the Arabidopsis glycerophosphodiester phosphodiesterase (GDPD) family reveals a role
681 of the plastid-localized AtGDPD1 in maintaining cellular phosphate homeostasis under
682 phosphate starvation. Plant J **66**: 781–95

683 **Dietz K-J** (2015) Efficient high light acclimation involves rapid processes at multiple
684 mechanistic levels. J Exp Bot **66**: 2401–14

685 **Dietz K-J, Heber U** (1986) Light and CO2 limitation of photosynthesis and states of the
686 reactions regenerating ribulose 1,5-bisphosphate or reducing 3-phosphoglycerate.
687 Biochim Biophys Acta - Bioenerg **848**: 392–401

688 **Dietz K-J, Turkan I, Krieger-Liszkay A** (2016) Redox- and Reactive Oxygen Species-
689 Dependent Signaling into and out of the Photosynthesizing Chloroplast. Plant Physiol **171**:
690 1541–50

691 **Dietz K, Heber U** (1984) Rate-limiting factors in leaf photosynthesis. I. Carbon fluxes in the
692 calvin cycle. Biochim Biophys Acta - Bioenerg **767**: 432–443

693 **Dietz KJ, Foyer C** (1986) The relationship between phosphate status and photosynthesis in
694 leaves : Reversibility of the effects of phosphate deficiency on photosynthesis. Planta **167**:
695 376–81

696 **Dong J, Ma G, Sui L, Wei M, Satheesh V, Zhang R, Ge S, Li J, Zhang T-E, Wittwer C, et**
697 **al** (2019) Inositol Pyrophosphate InsP8 Acts as an Intracellular Phosphate Signal in
698 Arabidopsis. Mol Plant **12**: 1463–1473

699 **Fabiańska I, Bucher M, Häusler RE** (2019) Intracellular phosphate homeostasis - A short
700 way from metabolism to signaling. Plant Sci **286**: 57–67

701 **Figueroa CM, Asencion Diez MD, Ballicora MA, Iglesias AA** (2022) Structure, function,
702 and evolution of plant ADP-glucose pyrophosphorylase. Plant Mol Biol **108**: 307–323

703 **Frank A, Matiolli CC, Viana AJC, Hearn TJ, Kusakina J, Belbin FE, Wells Newman D,**
704 **Yochikawa A, Cano-Ramirez DL, Chembath A, et al** (2018) Circadian Entrainment in
705 Arabidopsis by the Sugar-Responsive Transcription Factor bZIP63. Curr Biol **28**: 2597-
706 2606.e6

707 **Hammond JP, White PJ** (2008) Sucrose transport in the phloem: integrating root responses to
708 phosphorus starvation. J Exp Bot **59**: 93–109

709 **Hanchi M, Thibaud M-C, Légeret B, Kuwata K, Pochon N, Beisson F, Cao A, Cuyas L,**
710 **David P, Doerner P, et al** (2018) The Phosphate Fast-Responsive Genes PECP1 and

711 PPsPase1 Affect Phosphocholine and Phosphoethanolamine Content. Plant Physiol **176**:
712 2943–2962

713 **Härtel H, Dormann P, Benning C** (2000) DGD1-independent biosynthesis of extraplastidic
714 galactolipids after phosphate deprivation in Arabidopsis. Proc Natl Acad Sci U S A **97**:
715 10649–54

716 **Häusler RE, Heinrichs L, Schmitz J, Flügge UI** (2014) How sugars might coordinate
717 chloroplast and nuclear gene expression during acclimation to high light intensities. Mol
718 Plant **7**: 1121–1137

719 **Heinrichs L, Schmitz J, Flügge U-I, Häusler RE** (2012) The Mysterious Rescue of adg1-
720 1/tpt-2 - an Arabidopsis thaliana Double Mutant Impaired in Acclimation to High Light -
721 by Exogenously Supplied Sugars. Front Plant Sci **3**: 265

722 **Heldt HW, Rapley L** (1970) Specific transport of inorganic phosphate, 3-phosphoglycerate
723 and dihydroxyacetonephosphate, and of dicarboxylates across the inner membrane of
724 spinach chloroplasts. FEBS Lett **10**: 143–148

725 **Hendriks JHM, Kolbe A, Gibon Y, Stitt M, Geigenberger P** (2003) ADP-glucose
726 pyrophosphorylase is activated by posttranslational redox-modification in response to light
727 and to sugars in leaves of Arabidopsis and other plant species. Plant Physiol **133**: 838–49

728 **Hilgers EJA, Schöttler MA, Mettler-Altmann T, Krueger S, Dörmann P, Eicks M, Flügge**
729 **UI, Häusler RE** (2018) The combined loss of triose phosphate and xylulose 5-
730 phosphate/phosphate translocators leads to severe growth retardation and impaired
731 photosynthesis in arabidopsis thaliana tpt/xpt double mutants. Front Plant Sci **9**: 1–24

732 **Huang J, Zhao X, Chory J** (2019) The Arabidopsis Transcriptome Responds Specifically and
733 Dynamically to High Light Stress. Cell Rep **29**: 4186-4199.e3

734 **Klecker M, Gasch P, Peisker H, Dörmann P, Schlicke H, Grimm B, Mustroph A** (2014) A
735 Shoot-Specific Hypoxic Response of Arabidopsis Sheds Light on the Role of the
736 Phosphate-Responsive Transcription Factor PHOSPHATE STARVATION
737 RESPONSE1. Plant Physiol **165**: 774–790

738 **Kobayashi K, Awai K, Takamiya K, Ohta H** (2004) Arabidopsis type B
739 monogalactosyldiacylglycerol synthase genes are expressed during pollen tube growth and
740 induced by phosphate starvation. Plant Physiol **134**: 640–8

741 **König J, Muthuramalingam M, Dietz K-J** (2012) Mechanisms and dynamics in the

742 thiol/disulfide redox regulatory network: transmitters, sensors and targets. Curr Opin Plant
743 Biol **15**: 261–8

744 **Kumar V, Sharma A, Bhardwaj R, Thukral AK** (2019) Elemental Composition of Plants
745 and Multivariate Analysis. Natl Acad Sci Lett **42**: 45–50

746 **Kunz HH, Häusler RE, Fettke J, Herbst K, Niewiadomski P, Gierth M, Bell K, Steup M,**
747 **Flügge U-I, Schneider A** (2010) The role of plastidial glucose-6-phosphate/phosphate
748 translocators in vegetative tissues of Arabidopsis thaliana mutants impaired in starch
749 biosynthesis. Plant Biol (Stuttg) **12 Suppl 1**: 115–28

750 **Laisk A, Siebke K, Gerst U, Eichelmann H, Oja V, Heber U** (1991) Oscillations in
751 photosynthesis are initiated and supported by imbalances in the supply of ATP and
752 NADPH to the Calvin cycle. Planta **185**: 554–62

753 **Lei M, Liu Y, Zhang B, Zhao Y, Wang X, Zhou Y, Raghothama KG, Liu D** (2011) Genetic
754 and genomic evidence that sucrose is a global regulator of plant responses to phosphate
755 starvation in Arabidopsis. Plant Physiol **156**: 1116–30

756 **Li H, He K, Zhang Z, Hu Y** (2023) Molecular mechanism of phosphorous signaling inducing
757 anthocyanin accumulation in Arabidopsis. Plant Physiol Biochem **196**: 121–129

758 **Lin TP, Caspar T, Somerville C, Preiss J** (1988) Isolation and Characterization of a
759 Starchless Mutant of Arabidopsis thaliana (L.) Heynh Lacking ADPglucose
760 Pyrophosphorylase Activity. Plant Physiol **86**: 1131–5

761 **Liu Y, Xie Y, Wang H, Ma X, Yao W, Wang H** (2017) Light and ethylene coordinately
762 regulate the phosphate starvation response through transcriptional regulation of
763 PHOSPHATE STARVATION RESPONSE1. Plant Cell **29**: 2269–2284

764 **Liu Z, Wu X, Wang E, Liu Y, Wang Y, Zheng Q, Han Y, Chen Z, Zhang Y** (2022) PHR1
765 positively regulates phosphate starvation-induced anthocyanin accumulation through
766 direct upregulation of genes F3'H and LDOX in Arabidopsis. Planta **256**: 42

767 **MacNeill GJ, Mehrpouyan S, Minow MAA, Patterson JA, Tetlow IJ, Emes MJ** (2017)
768 Starch as a source, starch as a sink: the bifunctional role of starch in carbon allocation. J
769 Exp Bot **68**: 4433–4453

770 **Matiolli CC, Soares RC, Alves HLS, Abreu IA** (2022) Turning the Knobs: The Impact of
771 Post-translational Modifications on Carbon Metabolism. Front Plant Sci **12**: 781508

772 **Matiolli CC, Tomaz JP, Duarte GT, Prado FM, Del Bem LEV, Silveira AB, Gauer L,**

773 **Corrêa LGG, Drumond RD, Viana AJC, et al** (2011) The Arabidopsis bZIP gene
774 AtbZIP63 is a sensitive integrator of transient abscisic acid and glucose signals. Plant
775 Physiol **157**: 692–705

776 **Matsoukas IG, Massiah AJ, Thomas B** (2013) Starch metabolism and antiflorigenic signals
777 modulate the juvenile-to-adult phase transition in Arabidopsis. Plant Cell Environ **36**:
778 1802–11

779 **Maxwell K, Johnson GN** (2000) Chlorophyll fluorescence--a practical guide. J Exp Bot **51**:
780 659–68

781 **Misson J, Raghothama KG, Jain A, Jouhet J, Block MA, Bligny R, Ortet P, Creff A,**
782 **Somerville S, Rolland N, et al** (2005) A genome-wide transcriptional analysis using
783 Arabidopsis thaliana Affymetrix gene chips determined plant responses to phosphate
784 deprivation. Proc Natl Acad Sci U S A **102**: 11934–9

785 **Moore M, Vogel MO, Dietz KJ** (2014) The acclimation response to high light is initiated
786 within seconds as indicated by upregulation of AP2/ERF transcription factor network in
787 Arabidopsis thaliana. Plant Signal Behav **9**: 1–4

788 **Morcuende R, Bari R, Gibon Y, Zheng W, Pant BD, Bläsing O, Usadel B, Czechowski T,**
789 **Udvardi MK, Stitt M, et al** (2007) Genome-wide reprogramming of metabolism and
790 regulatory networks of Arabidopsis in response to phosphorus. Plant Cell Environ **30**: 85–
791 112

792 **Mustroph A, Boamfa EI, Laarhoven LJJ, Harren FJM, Albrecht G, Grimm B** (2006)
793 Organ-specific analysis of the anaerobic primary metabolism in rice and wheat seedlings.
794 I: Dark ethanol production is dominated by the shoots. Planta **225**: 103–14

795 **Nam H-I, Shahzad Z, Dorone Y, Clowez S, Zhao K, Bouain N, Lay-Pruitt KS, Cho H,**
796 **Rhee SY, Rouached H** (2021) Interdependent iron and phosphorus availability controls
797 photosynthesis through retrograde signaling. Nat Commun **12**: 7211

798 **Niewiadomski P, Knappe S, Geimer S, Fischer K, Schulz B, Unte US, Rosso MG, Ache P,**
799 **Flügge UI, Schneider A** (2005) The Arabidopsis plastidic glucose 6-phosphate/phosphate
800 translocator GPT1 is essential for pollen maturation and embryo sac development. Plant
801 Cell **17**: 760–775

802 **Nilsson L, Lundmark M, Jensen PE, Nielsen TH** (2012) The Arabidopsis transcription factor
803 PHR1 is essential for adaptation to high light and retaining functional photosynthesis
804 during phosphate starvation. Physiol Plant **144**: 35–47

805 **Nilsson L, Müller R, Nielsen TH** (2007) Increased expression of the MYB-related
806 transcription factor, PHR1, leads to enhanced phosphate uptake in Arabidopsis thaliana.
807 Plant Cell Environ **30**: 1499–512

808 **Ohnishi M, Anegawa A, Sugiyama Y, Harada K, Oikawa A, Nakayama Y, Matsuda F,**
809 **Nakamura Y, Sasaki R, Shichijo C, et al** (2018) Molecular Components of Arabidopsis
810 Intact Vacuoles Clarified with Metabolomic and Proteomic Analyses. Plant Cell Physiol
811 **59**: 1353–1362

812 **Osorio MB, Ng S, Berkowitz O, De Clercq I, Mao C, Shou H, Whelan J, Jost R** (2019)
813 SPX4 Acts on PHR1-Dependent and -Independent Regulation of Shoot Phosphorus Status
814 in Arabidopsis. Plant Physiol **181**: 332–352

815 **Pant B-D, Pant P, Erban A, Huhman D, Kopka J, Scheible W-R** (2015a) Identification of
816 primary and secondary metabolites with phosphorus status-dependent abundance in
817 Arabidopsis, and of the transcription factor PHR1 as a major regulator of metabolic
818 changes during phosphorus limitation. Plant Cell Environ **38**: 172–87

819 **Pant BD, Burgos A, Pant P, Cuadros-Inostroza A, Willmitzer L, Scheible WR** (2015b) The
820 transcription factor PHR1 regulates lipid remodeling and triacylglycerol accumulation in
821 Arabidopsis thaliana during phosphorus starvation. J Exp Bot **66**: 1907–1918

822 **Paz-Ares J, Puga MI, Rojas-Triana M, Martinez-Hevia I, Diaz S, Poza-Carrión C,**
823 **Miñambres M, Leyva A** (2022) Plant adaptation to low phosphorus availability: Core
824 signaling, crosstalks, and applied implications. Mol Plant **15**: 104–124

825 **Preiss J** (1984) Starch, sucrose biosynthesis and partition of carbon in plants are regulated by
826 orthophosphate and triose-phosphates. Trends Biochem Sci **9**: 24–27

827 **Preiss J** (1988) Biosynthesis of starch and its regulation. *In* J Preiss, ed, Biochem. Plants, 14th
828 ed. Academic Press, San Diego, pp 181–254

829 **Puga MI, Mateos I, Charukesi R, Wang Z, Franco-Zorrilla JM, de Lorenzo L, Irigoyen**
830 **ML, Masiero S, Bustos R, Rodríguez J, et al** (2014) SPX1 is a phosphate-dependent
831 inhibitor of Phosphate Starvation Response 1 in Arabidopsis. Proc Natl Acad Sci U S A
832 **111**: 14947–52

833 **Ramaiah M, Jain A, Baldwin JC, Karthikeyan AS, Raghothama KG** (2011)
834 Characterization of the phosphate starvation-induced glycerol-3-phosphate permease gene
835 family in Arabidopsis. Plant Physiol **157**: 279–91

836 **Rawat R, Schwartz J, Jones MA, Sairanen I, Cheng Y, Andersson CR, Zhao Y, Ljung K,**
837 **Harmer SL** (2009) REVEILLE1, a Myb-like transcription factor, integrates the circadian
838 clock and auxin pathways. Proc Natl Acad Sci U S A **106**: 16883–8

839 **Ried MK, Wild R, Zhu J, Pipercevic J, Sturm K, Broger L, Harmel RK, Abriata LA,**
840 **Hothorn LA, Fiedler D, et al** (2021) Inositol pyrophosphates promote the interaction of
841 SPX domains with the coiled-coil motif of PHR transcription factors to regulate plant
842 phosphate homeostasis. Nat Commun **12**: 384

843 **Riemer E, Qiu D, Laha D, Harmel RK, Gaugler P, Gaugler V, Frei M, Hajirezaei M-R,**
844 **Laha NP, Krusenbaum L, et al** (2021) ITPK1 is an InsP6/ADP phosphotransferase that
845 controls phosphate signaling in Arabidopsis. Mol Plant **14**: 1864–1880

846 **Robinson S, Giersch C** (1987) Inorganic Phosphate Concentration in the Stroma of Isolated
847 Chloroplasts and Its Influence on Photosynthesis. Aust J Plant Physiol **14**: 451

848 **van Rooijen R, Harbinson J, Aarts MGM** (2018) Photosynthetic response to increased
849 irradiance correlates to variation in transcriptional response of lipid-remodeling and heat-
850 shock genes. Plant direct **2**: e00069

851 **Rubio V, Linhares F, Solano R, Martín AC, Iglesias J, Leyva A, Paz-Ares J** (2001) A
852 conserved MYB transcription factor involved in phosphate starvation signaling both in
853 vascular plants and in unicellular algae. Genes Dev **15**: 2122–33

854 **Sakuraba Y, Kanno S, Mabuchi A, Monda K, Iba K, Yanagisawa S** (2018) A phytochrome-
855 B-mediated regulatory mechanism of phosphorus acquisition. Nat plants **4**: 1089–1101

856 **Scheible W-R, Pant P, Pant BD, Krom N, Allen RD, Mysore KS** (2023) Elucidating the
857 unknown transcriptional responses and PHR1 mediated biotic and abiotic stress tolerance
858 during phosphorus-limitation. J Exp Bot **11**: erad009

859 **Schmitz J, Schöttler MA, Krueger S, Geimer S, Schneider A, Kleine T, Leister D, Bell K,**
860 **Flügge U-I, Häusler RE** (2012) Defects in leaf carbohydrate metabolism compromise
861 acclimation to high light and lead to a high chlorophyll fluorescence phenotype in
862 Arabidopsis thaliana. BMC Plant Biol **12**: 8

863 **Schneider A, Häusler RE, Kolukisaoglu Ü, Kunze R, Van der Graaff E, Schwacke R,**
864 **Catoni E, Desimone M, Flügge UI** (2002) An Arabidopsis thaliana knock-out mutant of
865 the chloroplast triose phosphate/phosphate translocator is severely compromised only
866 when starch synthesis, but not starch mobilisation is abolished. Plant J **32**: 685–699

867 **Schreiber U, Schliwa U, Bilger W** (1986) Continuous recording of photochemical and non-
868 photochemical chlorophyll fluorescence quenching with a new type of modulation
869 fluorometer. Photosynth Res **10**: 51–62

870 **Sivak MN, Walker DA** (1986) Photosynthesis in vivo can be limited by phosphate supply.
871 New Phytol **102**: 499–512

872 **Smith AM, Stitt M** (2007) Coordination of carbon supply and plant growth. Plant Cell Environ
873 **30**: 1126–49

874 **Stitt M, Grosse H** (1988) Interactions between Sucrose Synthesis and CO2 Fixation IV.
875 Temperature-dependent adjustment of the relation between sucrose synthesis and CO2
876 fixation. J Plant Physiol **133**: 392–400

877 **Stitt M, Wirtz W, Heldt HW** (1980) Metabolite levels during induction in the chloroplast and
878 extrachloroplast compartments of spinach protoplasts. Biochim Biophys Acta **593**: 85–
879 102

880 **Stitt M, Wirtz W, Heldt HW** (1983) Regulation of Sucrose Synthesis by Cytoplasmic
881 Fructosebisphosphatase and Sucrose Phosphate Synthase during Photosynthesis in
882 Varying Light and Carbon Dioxide. Plant Physiol **72**: 767–74

883 **Sun L, Song L, Zhang Y, Zheng Z, Liu D** (2016) Arabidopsis PHL2 and PHR1 Act
884 Redundantly as the Key Components of the Central Regulatory System Controlling
885 Transcriptional Responses to Phosphate Starvation. Plant Physiol **170**: 499–514

886 **Suzuki N, Devireddy AR, Inupakutika MA, Baxter A, Miller G, Song L, Shulaev E, Azad**
887 **RK, Shulaev V, Mittler R** (2015) Ultra-fast alterations in mRNA levels uncover multiple
888 players in light stress acclimation in plants. Plant J **84**: 760–72

889 **Thibaud M-C, Arrighi J-F, Bayle V, Chiarenza S, Creff A, Bustos R, Paz-Ares J, Poirier**
890 **Y, Nussaume L** (2010) Dissection of local and systemic transcriptional responses to
891 phosphate starvation in Arabidopsis. Plant J **64**: 775–89

892 **Vandenbussche F, Habricot Y, Condiff AS, Maldiney R, Van Der Straeten D, Ahmad M**
893 (2007) HY5 is a point of convergence between cryptochrome and cytokinin signalling
894 pathways in Arabidopsis thaliana. Plant J **49**: 428–441

895 **Vogel MO, Moore M, König K, Pecher P, Alsharafa K, Lee J, Dietz KJ** (2014) Fast
896 retrograde signaling in response to high light involves metabolite export, MITOGEN-
897 ACTIVATED PROTEIN KINASE6, and AP2/ERF transcription factors in Arabidopsis.

898 Plant Cell **26**: 1151–1165

899 **Wahl V, Ponnu J, Schlereth A, Arrivault S, Langenecker T, Franke A, Feil R, Lunn JE,**
900 **Stitt M, Schmid M** (2013) Regulation of flowering by trehalose-6-phosphate signaling in
901 Arabidopsis thaliana. Science **339**: 704–7

902 **Wang Z, Zheng Z, Song L, Liu D** (2018a) Functional Characterization of Arabidopsis PHL4
903 in Plant Response to Phosphate Starvation. Front Plant Sci **9**: 1432

904 **Wang ZQ, Zhou X, Dong L, Guo J, Chen Y, Zhang Y, Wu L, Xu M** (2018b) iTRAQ-based
905 analysis of the Arabidopsis proteome reveals insights into the potential mechanisms of
906 anthocyanin accumulation regulation in response to phosphate deficiency. J Proteomics
907 **184**: 39–53

908 **Ward JT, Lahner B, Yakubova E, Salt DE, Raghothama KG** (2008) The effect of iron on
909 the primary root elongation of Arabidopsis during phosphate deficiency. Plant Physiol
910 **147**: 1181–91

911 **Weise SE, Liu T, Childs KL, Preiser AL, Katulski HM, Perrin-Porzondek C, Sharkey TD**
912 (2019) Transcriptional Regulation of the Glucose-6-Phosphate/Phosphate Translocator 2
913 Is Related to Carbon Exchange Across the Chloroplast Envelope. Front Plant Sci **10**: 827

914 **Woodrow IE, Raymond Ellis J, Jellings A, Foyer CH** (1984) Compartmentation and fluxes
915 of inorganic phosphate in photosynthetic cells. Planta **161**: 525–30

916 **Wu FH, Shen SC, Lee LY, Lee SH, Chan MT, Lin CS** (2009) Tape-arabidopsis sandwich -
917 A simpler arabidopsis protoplast isolation method. Plant Methods **5**: 1–10

918 **Xu L, Zhao H, Wan R, Liu Y, Xu Z, Tian W, Ruan W, Wang F, Deng M, Wang J, et al**
919 (2019) Identification of vacuolar phosphate efflux transporters in land plants. Nat plants
920 **5**: 84–94

921 **Yu L, Fan J, Zhou C, Xu C** (2021) Chloroplast lipid biosynthesis is fine-tuned to thylakoid
922 membrane remodeling during light acclimation. Plant Physiol **185**: 94–107

923 **Zhou J, Jiao F, Wu Z, Li Y, Wang X, He X, Zhong W, Wu P** (2008) OsPHR2 is involved in
924 phosphate-starvation signaling and excessive phosphate accumulation in shoots of plants.
925 Plant Physiol **146**: 1673–86

926 **Zhu J, Lau K, Puschmann R, Harmel RK, Zhang Y, Pries V, Gaugler P, Broger L, Dutta**
927 **AK, Jessen HJ, et al** (2019) Two bifunctional inositol pyrophosphate
928 kinases/phosphatases control plant phosphate homeostasis. Elife **8**: 1–25

929 **Zirngibl M-E, Araguirang GE, Kitashova A, Jahnke K, Rolka T, Kühn C, Nägele T,**
930 **Richter AS** (2023) Triose phosphate export from chloroplasts and cellular sugar content
931 regulate anthocyanin biosynthesis during high light acclimation. Plant Commun **4**: 100423

932

933

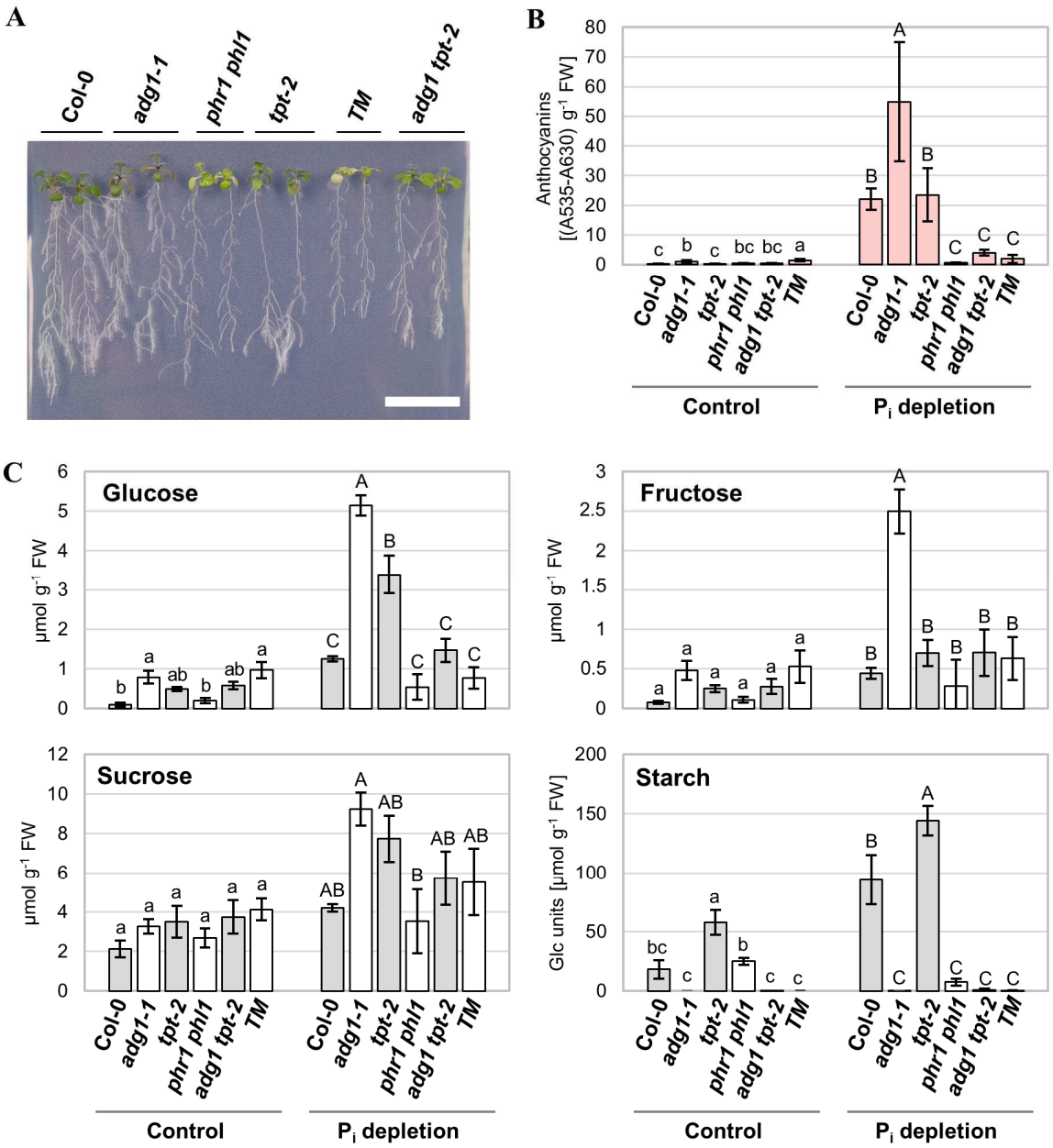

934

935 **Figure 1** P_i starvation responses are affected by photoassimilate partitioning. **A-C,** Seedlings
936 of wildtype (Col-0), *adg1-1*, *tpt-2*, *phr1-3 phl1*, *adg1 tpt-2* and *adg1 phr1-3 phl1* (**TM**)
937 genotype were grown for 7 (A), 5 (B), or 10 (C) days on rich medium including 0.5 % sucrose
938 before transfer to media with 0.5 % sucrose and either 2.5 mM (**Control**) or 0 mM (**P_i**
939 **depletion**) KH_2PO_4 added. Growth was continued for 8 (A), or 7 (B, C) days. **A,** Seedling
940 phenotypes under P_i deficient growth conditions. Bar, 2 cm. **B,** Anthocyanin contents of
941 seedling shoots. Pigment levels are depicted as units of absorbance (A535 - A630) relative to
942 shoot fresh weights. Bars represent means ± standard deviations; n = 5-6 pools of seedling
943 shoots from 3 independent experiments; **C,** Contents of glucose, fructose, sucrose and starch.
944 Pools of seedling shoots were harvested 10.25 hours after onset of the 16-hours photoperiod.

945 Means ± standard deviations; n = 3 independent experiments. **B, C,** Statistical analyses were
946 performed with One-way ANOVA with Tukey HSD follow-up test and Bonferroni alpha
947 correction for contrasts; P <0.05.

948

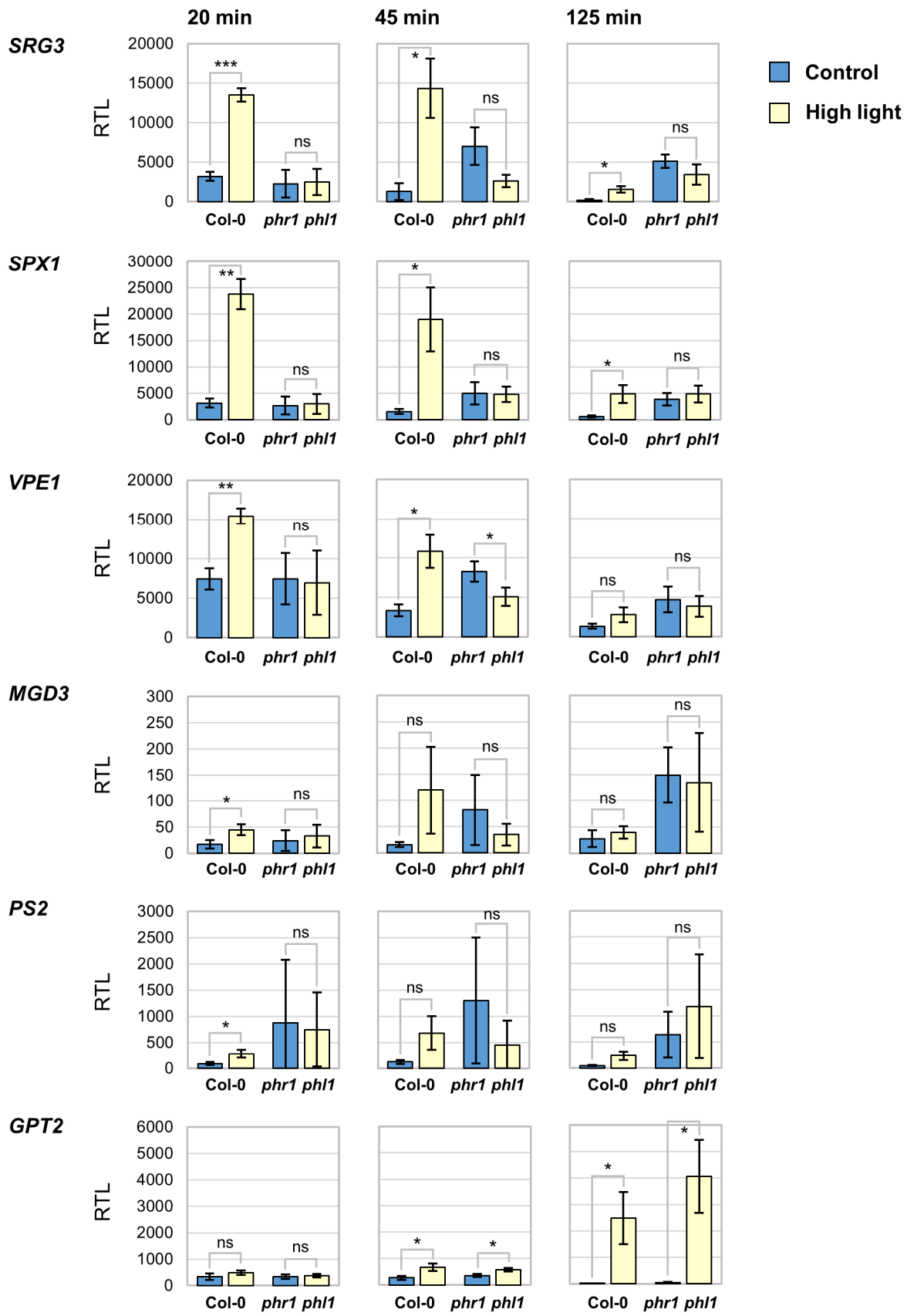

949

950 **Figure 2** PHR1-target genes are rapidly induced by high light. qRT-PCR analyses of indicated
951 transcripts in rosette leaves from wildtype (Col-0) and *phr1-1 phl1* mutants. Plants were grown
952 on soil for 5 weeks in an 8-hours light regime at 80±5 µmol m^{-2} s^{-1} before light intensity was

953 set to 320±30 µmol m^{-2} s^{-1} (High light, yellow bars) starting 1 hour after onset of the
954 photoperiod on day 36. The control group was kept at 80±5 µmol m^{-2} s^{-1} (blue bars). Per sample,
955 2-3 fully developed leaves (leaves no. 10-13) were harvested at the indicated treatment times.
956 Transcript levels were calculated relative to *PP2A* as $1000 \cdot 2^{-\Delta CT}$. Bars represent means
957 ± standard deviations, n = 3 independent experiments. Statistical analyses were performed
958 using Student's t test with 2-tailed distribution, unpaired with unequal variance. Significant
959 differences are indicated as ***P <0.001, **P <0.01, *P <0.05, ns, not significant.

960

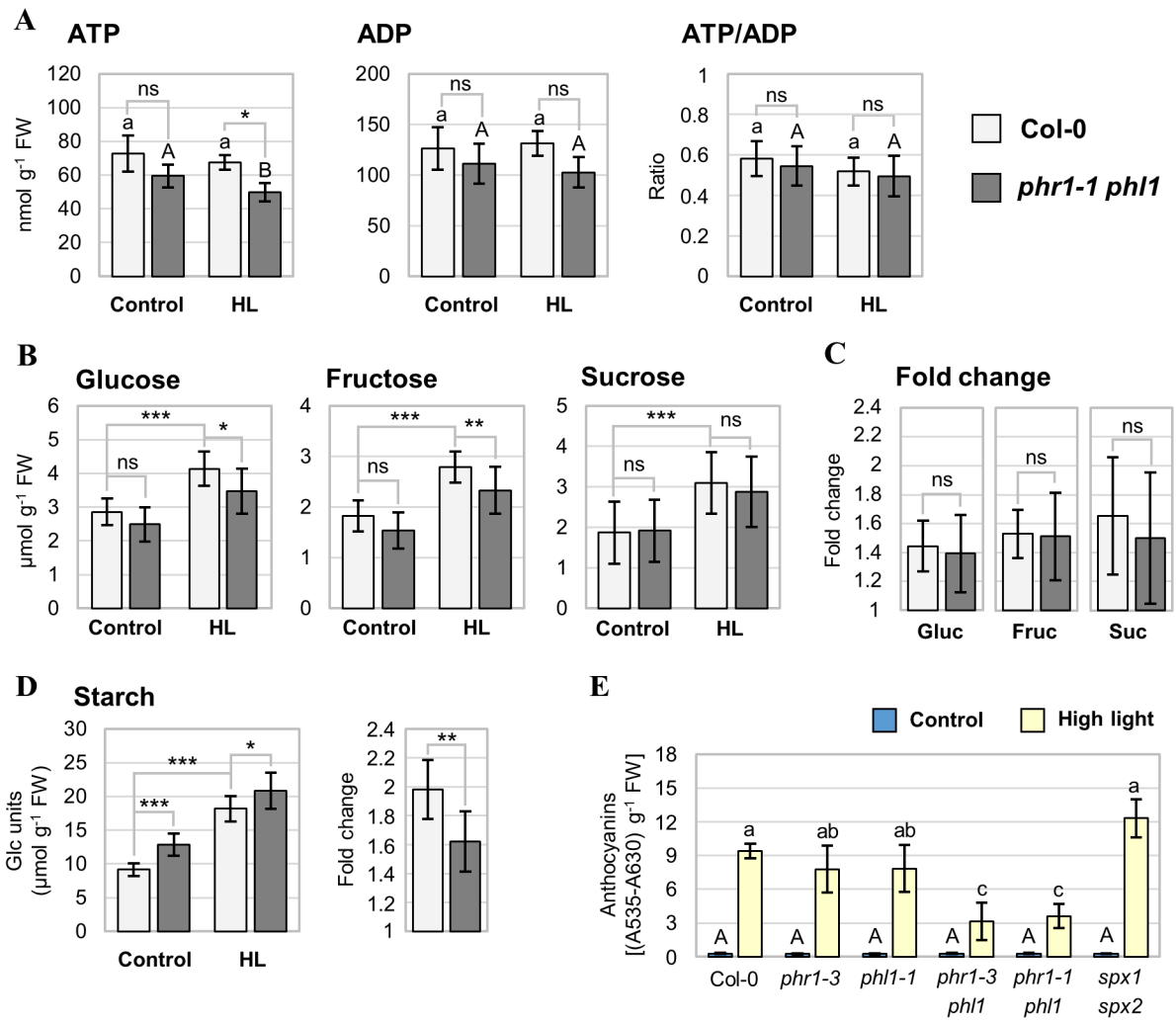

Figure 3 High-light induced metabolic changes in *phr1-1 phl1*. **A-D,** Levels of the indicated metabolites in leaves of wildtype (Col-0, light grey bars) and *phr1-1 phl1* mutants (dark grey bars) are depicted. Plants were grown and treated as described in Figure 2. Fully expanded leaves were sampled after 90 min of exposure to a photon flux density of either 80±5 µmol m^{-2} s^{-1} (**Control**) or 320±30 µmol m^{-2} s^{-1} (**HL**). Bars show means ± standard deviations; statistical analyses were performed with Student's *t* test with two-tailed distribution, unpaired with unequal variance. Significant differences are indicated as *** P <0.001, ** P <0.01, * P <0.05, ns not significant. **A,** n = 6 plants from 3 independent experiments; significant differences indicated by letter code: P <0.05. **B, C,** n = 11-12 plants from 4 independent experiments. **C, D,** Fold changes of sugar/starch contents were calculated for each genotype as HL/mean of control. **Gluc** glucose; **Fruc** fructose; **Suc** sucrose. **D,** n = 9 plants from 3 independent experiments. **E,** Anthocyanin levels determined in leaves of the indicated genotypes after 3 days of high-light exposure. Plants were grown for 32 days under low light conditions (70±10 µmol m^{-2} s^{-1}) in an 8-hours light regime. Subsequently, light intensity was increased for the treatment group (High light, yellow bars) to 450±30 µmol m^{-2} s^{-1}, while the

977 control group (blue bars) was kept under growth light conditions. Leaf material was harvested
978 after additional 70 hours. Pigment contents are expressed as absorbance units (A535 - A630)
979 relative to shoot fresh weight. n = 3 independent experiments; statistical analyses were
980 conducted using One-way ANOVA with Tukey HSD follow-up test and Bonferroni alpha
981 correction for contrasts, P <0.01; ns, not significant.

982

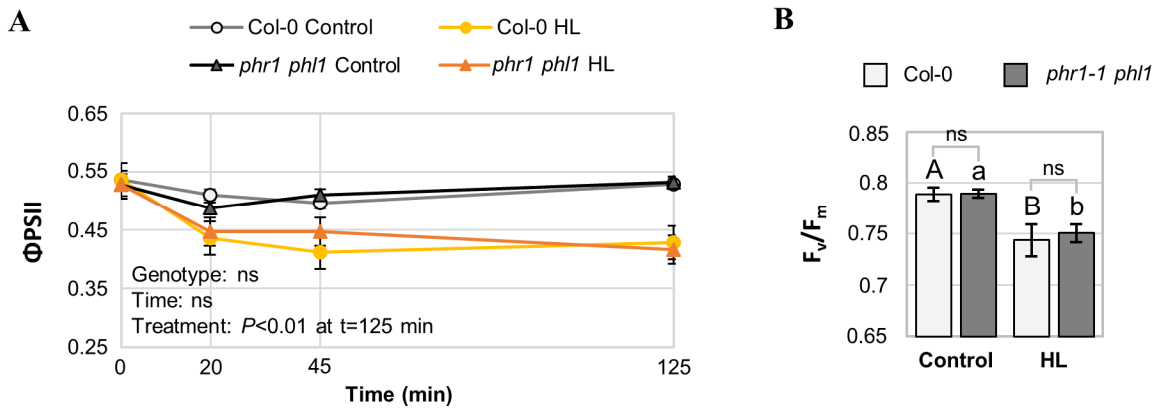

983

984 **Figure 4** Effect of high light on chlorophyll fluorescence in the *phr1-1 phl1* mutant. Plants of
985 wildtype (Col-0) and *phr1-1 phl1* genotype were grown as described in Figure 2. After 5 weeks
986 of growth, the light intensity was increased to 320±30 µmol m^{-2} s^{-1} for high-light (**HL**)
987 treatments, whereas the control group was kept under growth light conditions
988 (80±5 µmol m^{-2} s^{-1}). n = 3 independent experiments (representing means of each 3 leaves
989 measured). Significance was tested using One-way ANOVA with Tukey HSD follow-up test
990 and Bonferroni alpha correction for contrasts; ns, not significant. **A,** PAM measurements were
991 performed to determine the quantum yield of photosystem II photochemistry (ΦPSII) on light-
992 adapted leaves after 20, 45, and 125 min of treatment. **B,** Plants subjected to high-light stress
993 were dark-adapted for 20 min after 125 min of stress duration to determine the maximum
994 efficiency of photosystem II (F_v/F_m). Bars show means ± standard deviations; P <0.01.

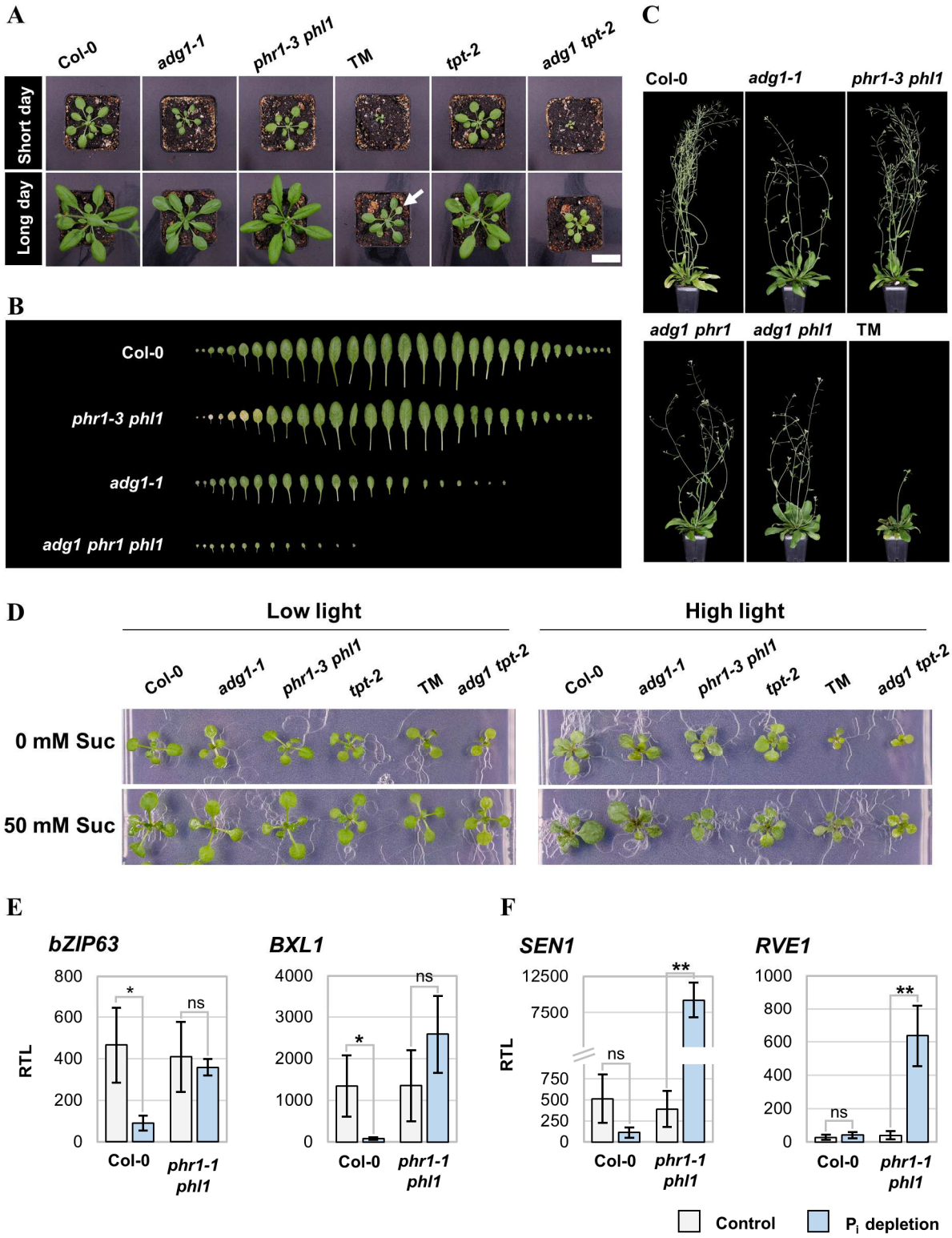

Figure 5 Carbohydrate metabolism is affected by *phr1 phl1* mutation. **A-D,** Phenotypes of the *adg1 phr1 phl1* triple mutant (**TM**). **A-C**, Plants were grown at 23°C and a light intensity of 100±10 µmol m^{-2} s^{-1}. **A,** Rosette habitus of plants grown under short-day (8 hours light period) and long-day (16 h light period) conditions. Pictures were taken of representative plants after 27 (short day) and 25 (long day) days of growth. The arrow indicates a senescent leaf. Bar,

1001 2.5 cm. **B,** Leaves of 42 day-old plants grown under an 8-hours light regime were aligned
1002 according to age (starting with the cotyledons on the left hand side). **C,** Inflorescences of
1003 wildtype (Col-0), *adg1-1*, *phr1-3 phl1*, and derived genotypes showing delay of the transition
1004 to flowering in the TM. Pictures were taken of representative plants after 42 days of growth
1005 under a 16-hours light regiment. **B, C,** Backgrounds were manually removed for better
1006 visualization. **D**, High-light sensitivity of TM and growth promotion by exogenous sucrose.
1007 Seedlings were grown in long-day conditions under low light (50±5 µmol m^{-2} s^{-1}) or high light
1008 (320±30 µmol m^{-2} s^{-1}) on rich media with or without sucrose added. Media-containing square
1009 petri dishes were positioned horizontally. Pictures were taken after 14 days of growth. **E, F**,
1010 Carbohydrate responsive gene expression is affected under P_i starvation. qRT-PCR analysis of
1011 carbohydrate-responsive transcripts which are downregulated in shoots of the wildtype (E), or
1012 upregulated in shoots of *phr1-1 phl1* mutant seedlings (F) grown for 7 days on rich medium
1013 containing 0.5 % sucrose, and for additional 8 days on media with 0.5 % sucrose and either
1014 2.5 mM (control, light grey bars), or 0 mM (P_i depletion, blue bars) KH_2PO_4 added. Transcript
1015 levels were calculated relative to the level of *PP2A* transcript as $1000 \cdot 2^{-\Delta CT}$. Bars represent
1016 means ± standard deviations; n = 3 independent experiments. One-way ANOVA with Tukey
1017 HSD follow-up test and Bonferroni alpha correction for contrasts; ** P <0.01, * P <0.05, ns,
1018 no significant difference.

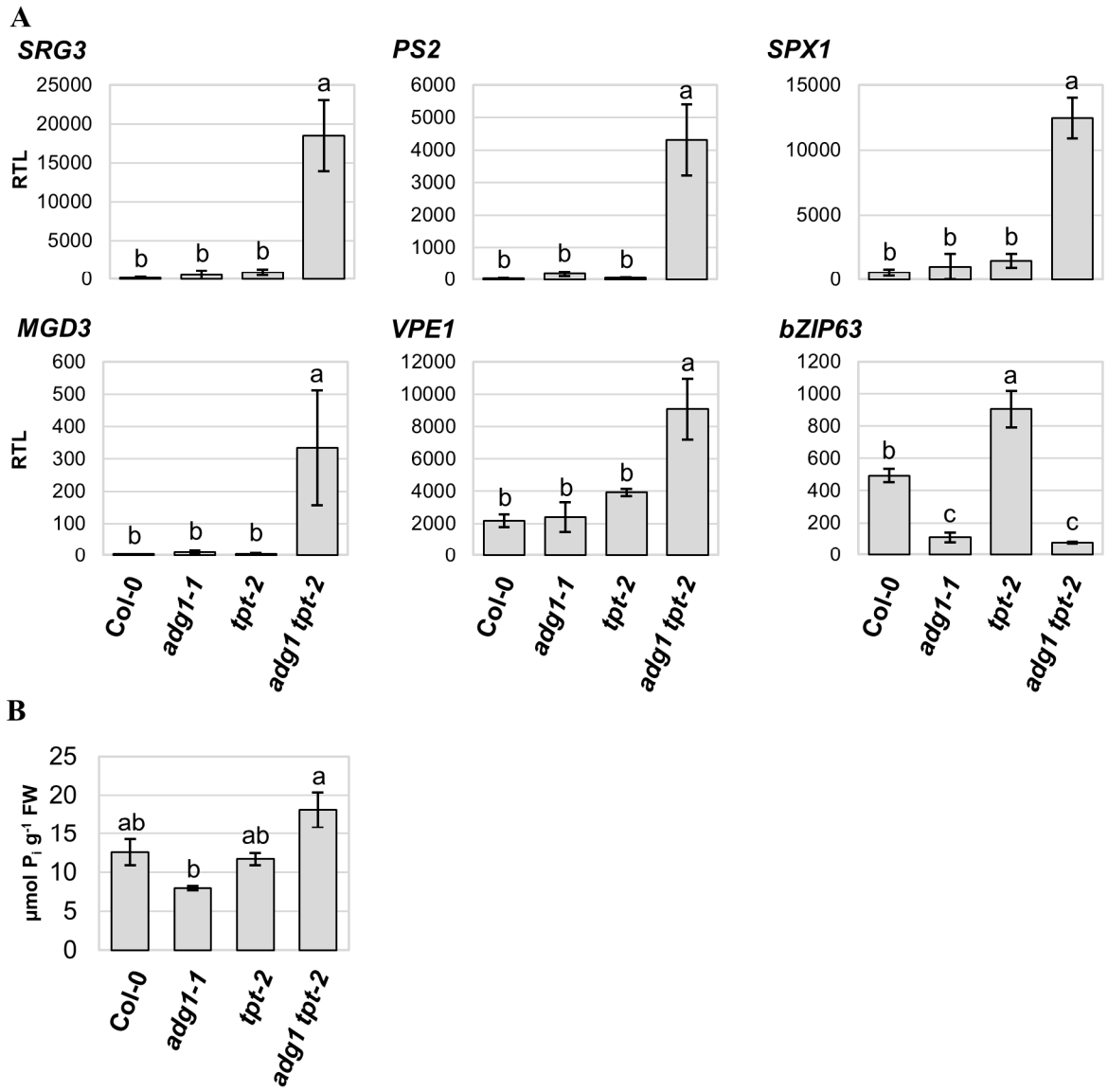

1019

1020 **Figure 6** Constitutive P_i starvation transcription in rosette leaves of *adg1 tpt-2*. **A, B,** Plants
1021 were grown on soil at a photon flux density of 90±10 µmol m^{-2} s^{-1} and sampled 135 min after
1022 onset of the 8-hours photoperiod after 5 weeks of growth. **A,** qRT-PCR analysis of the transcript
1023 levels of P_i starvation marker genes in rosette leaves of wildtype (Col-0), *adg1-1*, *tpt-2*, and
1024 *adg1 tpt-2*. Transcript levels are $1000 \cdot 2^{-\Delta CT}$ relative to *PP2A*. Bars show means ± standard
1025 deviations. n = 3 independent experiments. One-way ANOVA with Tukey HSD follow-up test
1026 and Bonferroni alpha correction for contrasts; P <0.01. **B,** P_i contents of rosette leaves. Means
1027 ± standard deviations are depicted. n = 3 independent experiments. Kruskal-Wallis test with
1028 DUNN's follow-up test and DUNN/Sidak alpha correction for contrasts; P <0.01.

1029

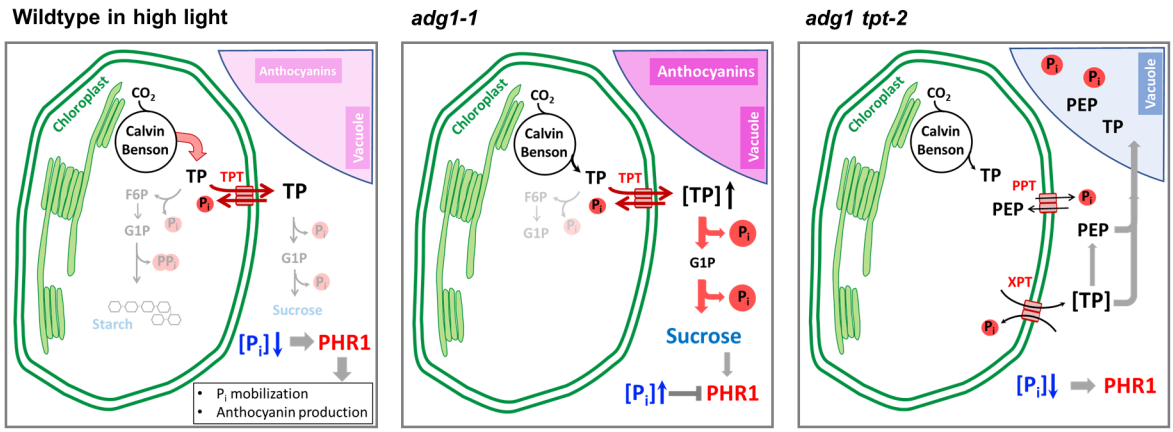

1030

1031 **Figure 7** Model for PHR1 activation during imbalances in triose phosphate production and
1032 consumption. In wildtype mesophyll cells subjected to an increase in light intensity (left panel),
1033 triose phosphate (TP) production by the Calvin-Benson-Bassham cycle transiently exceeds the
1034 rates of TP utilization by starch and sucrose biosynthesis causing sequestration of free P_i.
1035 Increased export of TPs to the cytosol via the TPT leads to a decrease in P_i concentration in the
1036 cytosol which results in PHR1 activation. High PHR1 activity facilitates the mobilization of P_i
1037 from internal sources including the stimulation of starch accumulation, and, together with a
1038 signal derived from TPs or 3-phosphoglycerate (3-PGA) accumulation, PHR1 triggers
1039 anthocyanin production. In the *adg1-1* knockout (middle panel), TPs accumulate in the cytosol
1040 due to the lack of starch biosynthesis. High TP/3-PGA levels in the cytosol promote
1041 anthocyanin production and sucrose biosynthesis. High sucrose levels enhance P_i-starvation
1042 responses (Lei et al., 2011), while TP turnover confined to the cytosol keeps PHR1 activation
1043 at a moderate level. In *adg1 tpt-2* (right hand side panel), TP export relies on the xylulose
1044 5-phosphate/P_i translocator (XPT) (Hilgers et al., 2018), keeping sucrose biosynthesis at low
1045 levels (Schmitz et al., 2012). TPs are partially consumed by glycolysis and imported back into
1046 the chloroplast by the phosphoenolpyruvate (PEP)/P_i translocator (PPT). Another portion of
1047 TPs and PEP is transferred to the vacuole where P_i is released by phosphatase activity.
1048 However, overall release of free P_i in the cytosol is low thus keeping PHR1 activity at high
1049 levels.